Decoding Gating Properties of the Pannexin1 Channel:

ATP Release and pH Sensitivity and the Potential Role

in Health and Disease

Paige Alexandra Whyte – Fagundes

A THESIS SUBMITTED TO THE FACULTY OF GRADUATE STUDIES
IN PARTIAL FULFILLMENT OF THE REQUIREMENTS
FOR THE DEGREE OF

MASTER OF SCIENCE

Graduate Program in Biology

York University
Toronto, Ontario
August 2015

Abstract

Panx1 is implicated in disorders including epilepsy and ischemia, with roles in important physiological processes including learning, memory and sensory function. In sensory systems, ATP release and purinergic signaling is considered the most important function of Panx1. Here, the function in the olfactory epithelium was investigated using Panx1 knock out mice. Functional analysis *in vivo* confirmed a role in olfaction suggesting that Panx1 is one of several alternative ATP release pathways. Since epileptic and ischemic events cause extracellular pH changes, the role of Panx1 in pH sensing was explored next. In a cell model Panx1 showed pH dependent channel gating properties. Site directed mutagenesis and high throughput dye uptake tests revealed a conserved domain of the protein as a pH sensor. Further, the critical role of a single histidine residue in this domain was determined. In summary, these studies demonstrate the role of Panx1 in ATP release and pH sensing.

Preface

Results of chapters 4 are published in a peer-reviewed journal

- Chapter 4: Kurtenbach, S., **Whyte-Fagundes**, **P**., Gelis, L., Kurtenbach, S., Brazil, E., Shestopalov, I., Hatt, H., Zoidl, G. (2014) Investigation of olfactory function in a Panx1 knock out mouse model. *Frontiers in cellular neuroscience*, *8*, 1-8.

Manuscript in preparation

- **Whyte-Fagundes, P**., Zoidl, G (2015) Decoding unique gating properties of the pannexin1a channel using pH sensitivity models

Several co-authors have contributed directly in performing experiments and/or collecting data, and assisting in interpretation.

- Dr. Stefan Kurtenbach furnished me with the tools to complete chapter 4; including in lab training, mentoring, and performing experiments by my side.
- Christiane Zoidl aided in tissue culture training and the development of the G418 panx1a/eyfp stable cell line.
- Dr. Silvia Penuela (Western University) provided an anti-Panx1 antibody
- Samille Oliveira Goncalves was responsible for conducting the fluorescent dye uptake assay completed by confocal microscopy

I performed all of the other experiments included in this body of work, and I was responsible for the writing of this manuscript.

Dedication

I dedicate this work to those individuals around me that are in the crossfire of multiple nonsensical conversations about the hours put into lab work and computer analysis, to hearing me rant about the trials and tribulations of graduate student life, and especially to those that deal with the, 'I can't I have to write my thesis' – aka my mother whenever she asked me to clean. I most definitely must pay a mention to my dance teacher, Sheila Graham, who always reminds me to prove myself to those who doubt me. I especially focus this dedication towards my mother and father, Gillian and Zeke, who directly and indirectly pushed and inspired me towards pursuing further education at my own discretion; and for forever providing me with the tools and support needed to succeed. Of course this dedication is not complete without the acknowledgement of my sisters, Hannah and Lydia, as they are each huge reasons for shaping me into the person I am today.

- Forever trying to do you all proud <3

ZF

Acknowledgments

"What you do makes a difference, and you have to decide what kind of difference you want to make."

- Jane Goodall

As Jane Goodall so eloquently puts, how you act as an individual effects those around you, and those that you choose to surround yourself with effects how you act. The relationships and friendships shaped over the past 2 years will stay with me for as long as I can remember. To begin, my special thanks are devoted to Dr. Georg Zoidl for many things beyond being a wonderful supervisor. Primarily, for being the only professor I interviewed with who didn`t tell me I had to give up on my extracurricular dreams to succeed at science, also for always being full of enthusiasm, support and encouraging words – my personal favourite, "every result is a result, even if it's a negative one." Not to mention all of the teasing he likes to do, as well as the advice and fruitful discussions we shared, along with having the possibility to develop my own ideas. Thanks for proofreading and making this thesis possible and allowing me to take risks. My sincerest hope is that this completed work is only the tip of the iceberg, and that future work continues to bear fruit for you in the future. Thank you Christiane for all of your tremendous technical help in the lab, I truly take 'the way of the Germans' for granted and have learned to love the organization. The lab would not be the well-oiled ship that it is without captain CZ, thank you for all of your patience and attempts at teaching me German! I sincerely appreciate the warm welcoming environment that has been provided by both of the Zoidls, from birthday cakes, to celebratory cakes, to the constant support I have witnessed for students that have moved on to future endeavours. I much appreciate the co-supervisory role that Dr. Donaldson has truly embodied; you truly inspired me to appreciate structural biology - sometimes. Extreme thanks to my in (and out of) lab mates, those who have moved on (Stefan and Sarah Kurtenbach – you two will always keep a special place in my heart, to whom I owe a lot of my lab successes to) and those that have stuck around for the long haul (Cherie brown, Ryan Siu), your constant enthusiasm for science, life, and online shopping (Cherie ;)) has really kept me going through the tough times. Ryan I appreciate all of the clarification and help you provide me in understanding things in the lab, not to mention your constant gerbil duty to

stores – saving me from having to go ☺. Cherie, girl, we both know this couldn't be done without each other. I could not ask or dream of a better cheerleader, gym buddy, and best friend <3. Thank you to all of my close friends at dance, who have now become sisters to me and were there to help keep me sane or fuel my insanity. Most importantly my family requires the most appreciation. My dad Zeke left us too soon, but I know he would be proud of this accomplishment and I will forever love you to the moon and back. Gillian, otherwise known as Mum, thank you for being the wonder woman that you are and inspire me to be. Hannah, you are a tough cookie and work so hard, always challenging me to do the same. Lydstone – well, "Good morning, Good morning! Today is going to be a great day, and do you know why? – because every day is a great day.' Love you all to bits. Last but not least, I must acknowledge the lab Keurig for providing me with a constant stream of $C_8H_{10}N_4O_2$ and getting me through insurmountable amounts of long days and sleepless nights.

Table of Contents

List of Abbreviations

A	Alanine
AA	Amino Acid(s)
ACSF	Artificial cerebral spinal fluid
ATP	Adenosine-5’-triphosphate
BFA	Brefeldin A
BSA	Bovine serum albumin
C	Cysteine
Ca^{2+}	Calcium
cDNA	Complimentary DNA
CL	Cytoplasmic loop
CT	Carboxy terminus
Cx	Connexin
CNS	Central nervous system
DTT	Dithiothreitol
E	Glutamate
EGFP	Enhanced green fluorescent protein
EL	Extracellular loop
ER	Endoplasmic reticulum
EtBr	Ethidium bromide
EYFP	Enhanced yellow fluorescent protein
FBS	Fetal bovine serum
Gly0	Unglycosylated Panx1 protein species
Gly1	High mannose Panx1 protein species
Gly2	Complex glycosylated Panx1 protein species
H	Histidine
IHC	Immunohistochemistry

Inx	Innexin
K	Lysine
K^+	Potassium
KO	Knockout
mRNA	Messenger RNA
N	Asparagine
N2a	Neuroblastoma 2a or Neuro2a
NCBI	National center for Biotechnology Information
NGS	Normal goat serum
OB	Olfactory bulb
OR	Olfactory receptor
OSN	Olfactory sensory neuron
OE	Olfactory epithelium
ON	Over night
P2X-R	P2X receptor
P2Y-R	P2y receptor
Panx (1,2,3)	Pannexin (1,2,3)
PBS	Phosphate buffered saline
PCR	Polymerase chain reaction
PNGase F	Peptide -N-Glycosidase F
qPCR	Quantitative PCR
RT	Room temperature
TM	Transmembrane
VNO	Vomeronasal organ
WT	Wild type

List of Tables

List of Figures

Chapter 1

Introduction

`` Science makes people reach selflessly for truth and objectivity; it teaches people to accept reality, with wonder and admiration, not to mention the deep awe and joy that the natural order of things brings to the true scientist.`

- Lise Meitner

Biological sciences in the twenty-first century face many challenges with respect to integrating the understanding of structural properties with the dynamics of complex protein networks that make up living organisms. It has become evident that cell membrane proteins have contributed in large part to our current understanding of the various networks that control the behaviour of cells, and in turn, their contribution to organismal functioning (Folkow, 1994). However, there are many elements of cellular physiology that still have yet to be entirely comprehended both structurally and mechanistically. Nonetheless, it has been well accepted that cells have the ability to communicate with neighbouring cells and respond to their environment via their malleable membrane properties; which is where the research in this thesis is primarily dedicated. This overarching reductionist perspective highlights the importance of identifying the myriad of DNA, proteins, and small molecules that define molecular properties and biological activities of the cell; as the first step to understanding how organisms function as a whole under both physiological and pathophysiological conditions. Progressing through the hierarchy of integrative physiological research perspectives; starting at a molecular, subcellular then cellular level, research continues at a local control level – characterized as different cell types joining into organs and organ systems, and then to a central nervous system (CNS) control level, which looks at somatomotor (behaviour and functioning), visceromotor (circulation and digestion) and hormonal (metabolism and electrolytes) aspects of research. Ultimately, bench work research perspectives are important for providing a strong platform for holistic scientists, who aim to study and understand complex systems. This in turn provides a means towards achieving a translational neuroscience perspective, which has been strongly favoured by researchers in recent years (Dahl & Keane, 2012). As these demands for bench-to-bedside

approaches increase, the ubiquitously expressed Pannexin1 (Panx1) protein exemplifies how it can be achieved. Therefore, this thesis demonstrates cellular and molecular approaches that were later shifted into a mammalian mouse model – demonstrating a translational perspective, to investigate the properties of the Panx1 cell membrane protein during sensory system functioning. Moreover, additional cellular and molecular techniques were investigated, with the purpose of working towards a translational neuroscience perspective to prospectively elucidate gaps in epilepsy and ischemia research.

1.1 The Central Nervous system: Neural Communications

The human brain is a complex organ, composed mainly of neurons and glial cells. Classically, cells have been defined as the basic building block of all living things; being the smallest independent unit within all multicellular organisms (Dermietzel, Hwang, & Spray, 1990). A cell adapts to the characteristics of the structure it composes, which ultimately conforms to the general order of the system in which it resides and functions within. In order for these individual components to function in a meaningful, cohesive manner, with regulated control and coordination of simultaneously occurring functions, the exchange of information both supra-, intra- and intercellularly is extremely pertinent (Dermietzel et al., 1990). A region in which this is of particular importance is the CNS, which encompasses the brain and spinal cord, where full functionality is reliant upon neurons – the primary communicating cells of the nervous system, and their synapses (Purves et al., 2004).

Neuronal communication is crucial for proper physiological processes like perception, voluntary movement, sensory processing, or learning. In addition, correct development and function of the CNS is established and maintained through neural communication and function, achieved by the ion and metabolite exchange between neurons and the extracellular medium. This in part, relies on cell membrane channels formed by pannexin proteins (Zoidl & Spray, 2014). However, disrupting this communication and the maintenance of healthy neurons is often a precursor for pathological disorders like epilepsy, Alzheimer's, ischemia, and Parkinson's disease; to name a few.

1.2 The Pannexin1 Protein

In the early 20th century, it was thought that the primary, and possibly only, form of allowing neuronal communication was via gap junctions. With the discovery of chemical communication, made possible by fundamental advances in physiology, this view changed and gap junction communication in the CNS was considered of less importance. Observing the first neuron specific connexin in 1998 (Condorelli et al., 1998) was the first of two important discoveries, driving the gap junction field to new horizons. The second key discovery was not until 15 years ago, when a novel family of gap junction like proteins, the pannexins, were identified (Bruzzone et al., 2003, 2005). At that time, only two families of gap junction proteins were known, the connexins (Cxs) and innexins (Inxs) form cell-to-cell channels and adhesions in numerous cell types (Dahl & Keane, 2012). Cxs are gap junction proteins that are chordate specific and have isolated representation in the genomes of vertebrates. Hence, the latter discovery of Inxs; which possess a similar structure allowing the formation of junctions in invertebrates specifically. Historically, Panxs were thought to be a second family of gap junction proteins in vertebrates. However, rather than acting as the competitive partner to Cxs, they were found to function as distinct aqueous pores between the intra- and extracellular space of cells. Although the Panx family consists of 3 similar members, since their discovery, a considerable amount of attention has been focused on the biochemical and functional properties of the Panx1 protein. Thus, much of the literature pertaining to this work will be reviewed in the following sections, although the other paralogues may be addressed in succession.

1.2.1 Discovery

In 2000, database research using a PSI-BLAST (Position Specific Iterative-Basic Local Alignment Search Tool) approach, a tool designed to search protein and DNA queries against databases for sequence similarities (Altschul et al., 1997), revealed two Inx-like proteins in the human genome when searching GenBank (Panchin et al., 2000). Specifically, two mRNA sequences with no previously assigned functions – MRS1 (GenBank accession number AF093239) and MRS1-related proteins (GenBank accession number AL022328), were identified (Bruzzone et al., 2003; Baranova et al., 2004). Despite the fact that the presence of four transmembrane domains is a

possible source of error during these sequence scans for homology, since there exists multiple tetra-spanning proteins like claudins and occludins that are unrelated to our proteins of interest (Fushiki et al., 2010), two well-conserved cysteine residues that are carboxy to the first transmembrane sequence were found in the new proteins. These were highlighted as sufficient indicators of homology based upon their location outside of the transmembrane regions. In addition, when an entire detailed sequence comparison was completed, researchers revealed only a 16% similarity amongst the Inx and Panx proteins. However, the investigation was narrowed to just the first extracellular loop and first two transmembrane segments, for true confirmation of homology. 60 amino acids were shown to be similar, including the conserved cysteine residues in the extracellular loop (Figure 1) and a proline motif in the second transmembrane segment. Similarity decreases when comparing the second half of the structure, seeing as that part of the Panx protein is much shorter than Inx, and any conserved regions seem to be displaced (Phelan, 2005). All in all, Panxs and Inxs seem to show extreme topological similarities, regardless of the little shared sequence relationship, which allows both of these proteins to associate into hexamers forming either homo- or heteromeric channels (Abascal & Zardoya, 2012).

The discovery of Panx was also engineered when Panchin et al (2000) cloned murine cDNA that encoded for an 'Inx-like' molecule from a fetal brain sample. Again, statistically significant similarities to invertebrate Inxs were found; including the conservation of the cysteines and transmembrane regions mentioned prior. Several studies since have statistically confirmed homology between Inxs and Panxs as well (Fushiki et al., 2010). However, based upon the discovery of the ubiquitous expression of Inx members in animal phyla, Panchin disputed the appropriateness of the Inx name (invertebrate analog of connexions, present in non-chordates) to be applied to all species. As a result, the emergence of the re-branded 'Panx' name came to be widely adopted for chordate animals; *pan* meaning 'complete' or 'all' and *nexus* meaning 'junction' or 'connection.' With time, MRS1 and MRS1-related proteins adopted the names Panx1 and its related isoform Panx2, respectively. It is important to note that following the identification of Panx1 and 2, a protein sequence query (TBLASTN) was applied against the human genome and the final Panx paralog, Panx3, was revealed (Bruzzone et al.,

2003). These three family members comprise the family of channel-forming glycoproteins. Whose function is defined by their ability to form single-membrane channels regulated by post-translational modifications, channel intermixing and sub-cellular expression; which will be discussed in further detail.

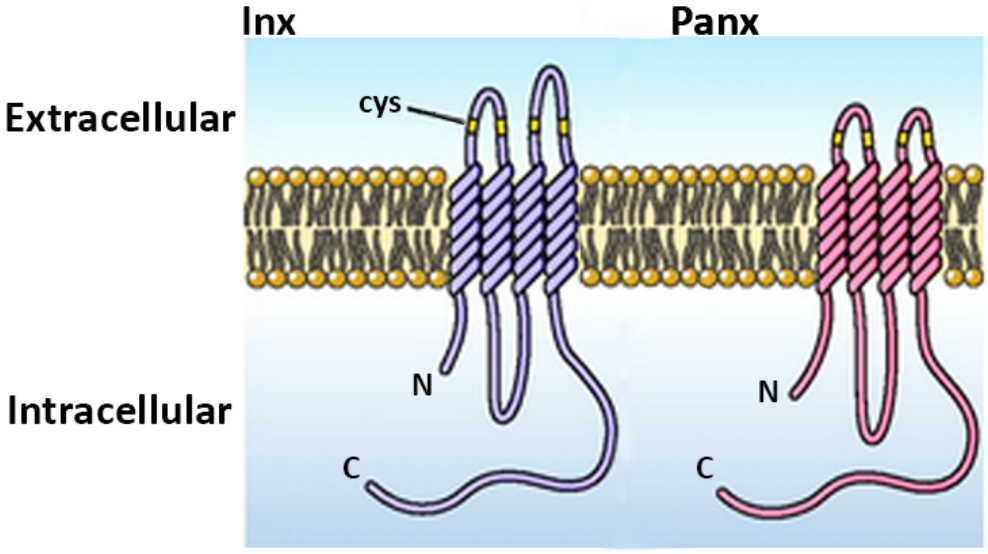

Figure 1: Comparative analysis of the membrane topology of innexins and pannexins. Schematic drawing depicting the predicted arrangement of one member of the Inx and Panx family relative to the plasma membrane. It is obvious that they both share topological similarities like the presence of four transmembrane regions, an amino (N) and carboxy (C) terminal, and are similar in size (in kDa: 48.9 and 48.1 for Inx and Panx respectively. Indicated in yellow, and labelled, are the equally spaced cysteine residues which are conserved within families; with only the first two residues being conserved between families. This image also depicts the difference in the length of the second extracellular loop between the two proteins. Figure modified and adapted from American Physiological Society. (Barbe, Monyer & Bruzzone, 2006).

1.2.2 Biochemical and structural properties

Panx orthologs have been found in vertebrate lines including human, mouse, rat and zebrafish (Panchin et al., 2000; Bruzzone et al., 2003). Experimentation conducted in this thesis specifically includes the use of Panx1 found in mouse (mPanx1: 426 residues long, 48.2kDa in size and located on chromosome 9) and Panx1a from zebrafish (drPanx1a: 417 amino acids, 46.9kDa, located on chromosome 15). The mouse (*Mus musculus)* and zebrafish (*Danio rerio)* models are ideal to use when studying the Panx1 protein because they have high similarity to humans; with mPanx1 having 83.84 and drPanx1a having 77.7 conserved nucleic acids compared to the commonly used frog (*Xenopus laevis)* model with only 74.25 similar nucleic acids (GeneCards®: The Human Gene Database). However, much of the pioneered research in Panx history was conducted in experiments using *Xenopus* oocytes.

Cxs, Inxs and Panxs can be thought of as protein cousins that possess overlapping functional properties with unique physiological roles. It is understood that Inxs form functional gap junctions in invertebrates and there is dated evidence to suggest the same of Panxs. This notion was widely accepted until approximately 2006, when Locovei et al (2006) found that Panx1 was present in erythrocytes; which do not typically form gap junctions in general. Further supporting evidence of non-gap junction functions of Panx1 include the fact that Panx1 is localized in the apical membrane of polarized cells, which do not exhibit cell-to-cell contact required to form gap junctions (Ransford et al., 2009). Additionally, immunohistological staining of Panx is different to that of gap junctions, which typically demonstrate plaque formations (Dahl & Locovei, 2006). Researchers also revealed that Panx1 is found asymmetrically distributed at synapses, with exclusive expression at the postsynaptic membrane, ruling out electrical synapse function that is native to gap junction proteins (Zoidl et al., 2007). In addition, Panxs have an important N-glycosylation site in the extracellular loops, present in all three homologs, that is capable of preventing efficient docking of two pannexons (Figure 2); which is necessary for gap junction channel formation (Boassa et al., 2007). In fact, experiments conducted by Boassa et al (2008) have shown that deglycosylating Panx1 with PNGase F results in increased intercellular coupling, indicative of gap junction formation. Therefore, researchers concluded that Panx channels must show similarity to the non-junctional type of channel that

Inxs can also form, functioning as unopposed hemichannels. Despite their low sequence homology, as mentioned prior, this non-junction function may be due to the similar topological features that are found between Inxs and Panxs. In particular, Panx1, like Inxs, resides structurally as a cell membrane protein with four transmembrane domains (TM1-TM4), two extracellular loops (EL1 and EL2), one intracellular loop (IL1) and an intracellular amino- and carboxy-terminal (N- and C-termini) (Bond & Naus, 2014) (Figure 3). To date, there have been no reported crystal structures of a Panx protein. However, methods like site-directed mutagenesis, have been employed to target specific residues within the sequence that are presumed to play a role in the tertiary/quaternary structure in order to predict how the 3D structure exists physiologically (Wang & Dahl, 2010) (Figure 2). Thus far, these analyses have revealed that there are four critical cysteines responsible for the formation of the channel; these pose as likely futuristic targets for investigating gating properties (Bunse et al., 2011).

1.2.2.2 Oligomerization

Early in Panx discovery, researchers presumed, and confirmed with electron microscopy, that the oligomerization of Panx1 was analogous to the hexameric Cx structure, 6 subunits to form a channel (Bruzzone et al., 2003). However, C-terminal truncated mutants have revealed that Panx2 likely assembles into heptamers or octomers, meanwhile, no oligomerization analysis for Panx3 is currently available – although, it is predicted to form hexamers (Penuela et al., 2013). Panx1 oligomers are typically referred to as pannexons, as Cxs are known as connexons. Prior to these pannexons trafficking to the cell surface, they oligomerize in the endoplasmic reticulum (ER) to form a hexamer and glycosylate at the extracellular surface (Peneula et al., 2009). Based on proper oligomerization of the protein, which is governed by the C-terminus along with glycosylation mediated cell surface trafficking (Gehi et al., 2011), there is compelling evidence to suggest that Panx paralogs intermix to form heteromeric pores in the membrane or remain homogenous to form homomeric channels (Penuela et al., 2013). Immunoprecipitation and co-expression experiments have both shown interactions between Panx1 and 2, and between Panx1 and 3; however, no interactions have been shown between Panx2 and 3. In particular, in situ hybridization has revealed co-expression of Panx1 and 2 in the pyramidal cells and

interneurons of the hippocampus and neocortex, olfactory bulb, pyramidal cells, dentate gyrus, and Purkinje cells of the cerebellum (Vogt, Hormuzdi, & Monyer, 2005). This co-expression seems to be governed by the level of N-glycosylation, seeing as only the core and high-mannose species of Panx1 co-immunoprecipitates with Panx2 (Penuela et al., 2009). Interestingly, research conducted in oocytes has revealed that this Panx1/2 co-expression does not appear to be conducive to channel activity or stability. Results showed that this configuration produces decreased channel currents, prolonged inactivation of the channels, and extended the period of time required to reach peak channel currents. In addition, it was found that Panx1/2 pannexons degrade much more rapidly than their monomeric counterparts (Ambrosi et al., 2010). Taken together, this suggests that Panx2 actually has an inhibitory effect on Panx1, which may or may not be due to the mis-trafficking or mis-folding of Panx1 in this heteromeric complex. However, there is also a possibility that Panx1/2 co-expression is non-functional (Ambrosi et al., 2010). That being said, it is undeniable how post-translational modifications are critical for channel oligomerization, as well as proper trafficking, intracellular localization and function of the Panx protein; which will be further discussed.

1.2.2.3 Posttranslational modifications

Posttranslational modifications of Panxs have demonstrated how important glycosylation of Panx1 is in terms of folding, stability, trafficking and function, in contrast to the phosphorylation patterns of Cxs (Boassa et al., 2007; Penuela et al., 2007). Boassa and Penuela et al (2007) showed that by blocking glycosylation, through targeting putative N-linked glycosylation sites via site directed mutagenesis or pharmacological agents, the ability of Panxs to transport to the plasma membrane is either reduced or abolished resulting in little to no cell surface expression. In fact, they were able to highlight one residue on Panx1, N254 or N246 in fish in EL2, which was of particular importance for proper glycosylation and targeting the hexamer to the membrane. As a result, it is proposed that *N*-glycosylation of Panx1 could be a significant mechanism for regulating trafficking of the membrane proteins to the cell surface in various cell types and tissues (Penuela et al., 2010). Interestingly, western blot experiments have revealed three distinct Panx1 species. The first form is the non-glycosylated core protein

known as Gly0, which has been shown to be resistant to glycosidase treatment. Gly1, which is the high mannose species, is predominant in the Endoplasmic Reticulum (ER) and is sensitive to endoglycosidase H treatments. Finally, Gly2 is glycosylated following movement from the ER to the Golgi apparatus, mediated by COPII vesicles (Bhalla-Gehi, Penuela, Churko, Shao, & Laird, 2010), to form the mature-type or complex glycoprotein (trans-Golgi glycosylated). Therefore, it is safe to say that Panx1 expression patterns differ based upon their level of glycosylation (Kurtenbach et al., 2013). However, it is important to note that glycosylation seems to only occur at sites located in the lumen of the ER, which correspond to the extracellular domain of the protein (Boassa et al., 2007). If the protein happens to be glycosylation-deficient it seems to be retained in intracellular compartments and in the ER, resulting in lower expression at the cell surface. Nonetheless, glycosylation deficiency does not seem to affect the folding of the protein subunits, i.e. – their ability to assemble into oligomers (Boassa, Qiu, Dahl, & Sosinsky, 2008). Therefore, the question left standing is, can Panxs form functional channels in the absence of glycosylation? There is limited research showing definitive results for this, however, it is clear that Panx1 clearly demonstrates unique kinetics and dynamics as a channel membrane protein.

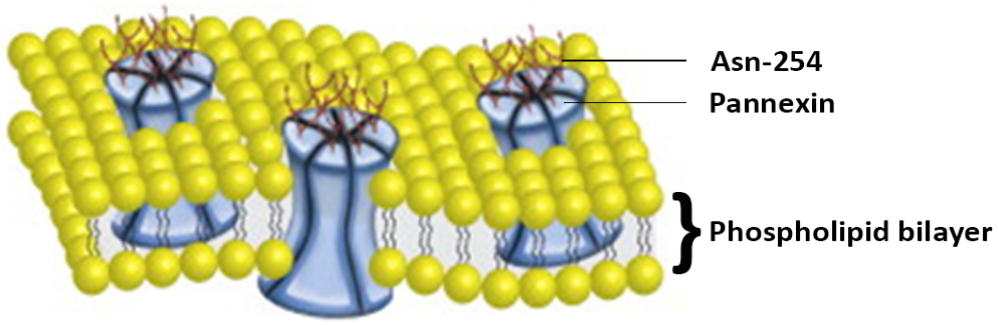

Figure 2: Pannexin channel formation in membrane. Six pannexin segments join in a homomeric, all Panx1, or heteromeric, Panx1 & 2, formation in the cell membrane. There is a glycosylation site indicated at N254 of Panx1, N86 & 71 in Panx2 & 3 respectively, which is responsible for docking into the membrane and preventing the formation of gap junction, leading to the formation of unopposed hemichannels. Figure adapted and modified from Biochimica et Biophysica Acta (BBA)- Biomembranes. (Penuela, Gehi & Laird, 2013).

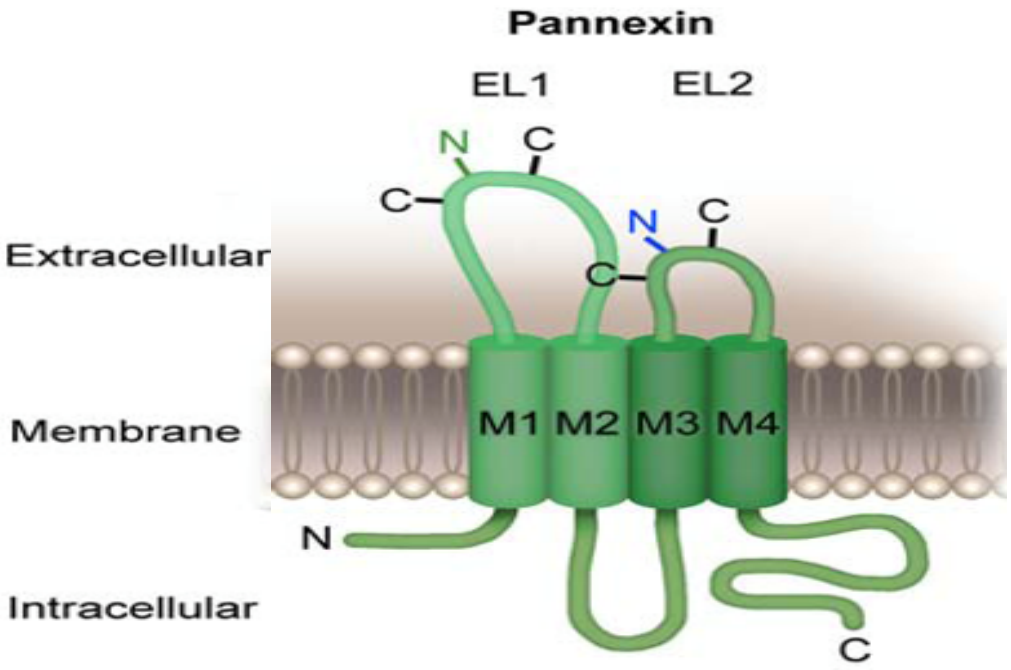

Figure 3: Depiction of the structural composition of the pannexin proteins, including Panx1. Topology of pannexin includes two extracellular loops (EL1 and EL2), four transmembrane segments (M1-4), as well as an intracellular amino (N) and carboxy (C) terminal. M1 and M2 are shown in a lighter shade of green to indicate the higher homology they share with innexins. While the "N" in the EL2 shown in blue, specifies the glycosylation site of Panx1 (and 2). Although Panx3 is not a highlight of this project, it is important to mention that the green "N" in EL1 is also responsible for glycosylation; indicating how N-glycosylation is a unique feature of the pannexin protein family. Figure modified from the Zoidl lab, artwork originally created by Helga Schulze.

1.2.2.4 Interacting Partners

There is a growing list of interacting partners with Panx1; implying how these varying protein complexes can play a dynamic and multifunctional role in cellular processes important for maintaining ion homeostasis and paracrine signaling. Key interacting partners for Panx1 include surface receptors and channels, whose interactions can be mediated by one of the following ways 1) interactions modulating intracellular Ca^{2+}; including NMDA, and P2X receptors, 2) interactions with Ca^{2+} mobilizing protein-coupled receptors such as P2Y, 3) and finally, interactions causing ATP signaling; including P2XRs and actin filaments (Figure 4).

Beyond the protein-protein interactions amongst Panx family members themselves, and the few interacting partners mentioned above, Panx1 has been shown to directly interact with actin at its C-terminal tail (Bhalla-Gehi et al., 2010). This interaction, between Panx1 CT and actin microfilaments specifically, is likely a factor that is responsible for proper trafficking and especially stability at the plasma membrane. This effect was speculated based upon observing the pharmacological disruption of the microfilaments displaying a reduction of cell surface stability and motility of Panx1 (Bhalla-Gehi et al., 2010). Panx1 has also been found to interact with P2X7 receptors, caspase-1, caspase-11, NLRP1, ASC and XIAP; which are all components of the inflammasome complex (Silverman et al., 2009). Unfortunately, research thus far has only identified these interactions, and has yet to consolidate the functional role Panx1 plays in the inflammasome (Penuela, Gehi, & Laird, 2013). However, the role is likely isolated to apoptotic events associated with cellular stress responses. P2XRs have been proposed as direct binding partners (Pelegrin & Surprenant, 2006). Beyond their interaction in the inflammasome complex, they also associate with Panx1 in response to extracellular ATP (Shestopalov & Slepak, 2014). The associations between Panx1 and the purinergic receptors will be discussed later in further detail, refer to figure 4 for a schematic of the interacting partners highlighted in this segment. It is important to note that only the partners of interest for Panx1, that are pertinent to this thesis, were mentioned while in reality there are many more. To conclude, it is obvious, by looking at some of the binding partners for one protein, that there is a complex network of interactions that occur at the level of the cell membrane. As a result, it is more than apparent that there is a significant chance of having compensatory mechanisms that override the study of specific molecular complexes, making the study of Panx1 in particular both difficult and fascinating.

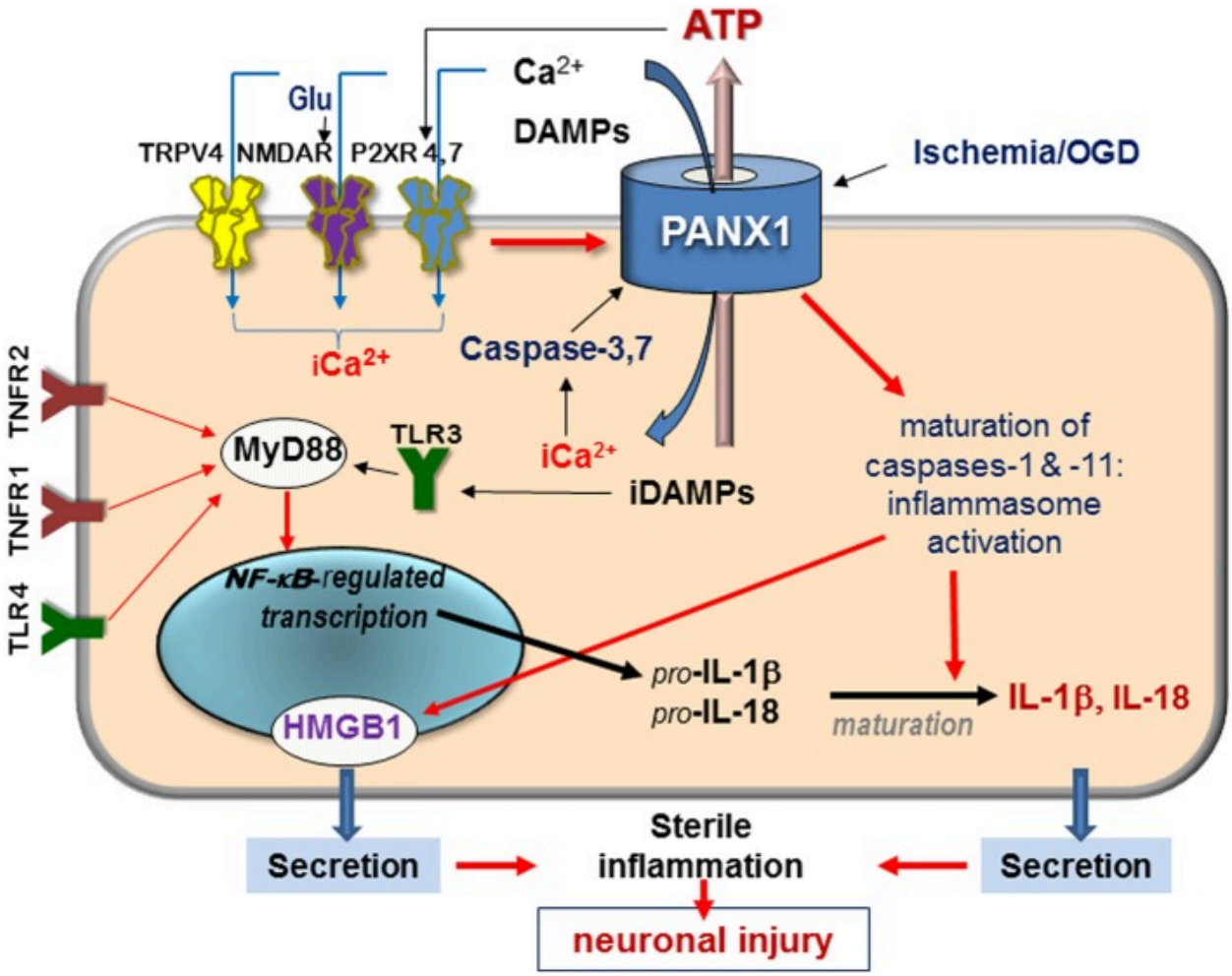

Figure 4: Diagram depicting signal mediated interacting proteins and receptors with Panx1. Panx1 channels open in response to elevated intracellular calcium (iCa2+) and allow a surge of calcium into the cell. Prolonged opening of Panx1 also causes a massive efflux of ATP. These 2 events are the leading cause of injury to the CNS. Caspase 3 and 7 with proteolysis can activate Panx1 also. There are indirect ways of activating Panx1 as well, through receptors and other channels. Purinergic receptors (P2XR) can mobilize intracellular calcium to activate the channel from the inside, ATP can bind onto these same receptors and activate Panx1. Finally, Glu (glutamate) can activate NMDARs and facilitate Panx1 opening too. It is important to note that red arrows denote activation pathways. Figure adapted and modified from Fronties in Physiology. (Shestopalov & Slepak, 2014).

1.2.3 Expression and distribution

Panx1 is ubiquitously expressed, forming channels in a variety of cell types and sensory systems, like the visual or olfactory system, during physiological and pathophysiological conditions, like intracellular calcium regulation and ischemia respectively. To exemplify the

importance of Panx1 as a protein, researchers have reported that it is expressed in most parts of the human body. Using *in situ* hybridization, northern blots, real time PCR, western blots and immunohistochemistry (IHC), temporally regulated expression of Panx1 has been revealed in the CNS (cerebellum, cortex, lens (fibre cells)), retina (retinal ganglion, amacrine and horizontal cells) (Ray et al., 2005), axon bundles of the olfactory epithelium (Kurtenbach et al., 2014), olfactory bulb, sensory cells of the vomeronasal organ, pyramidal cells, interneurons of the neocortex and hippocampus, amygdala, substantia nigra, neurons and glial cells. In addition, northern blot analysis has confirmed robust expression in the brain and variable levels of expression in other tissues and cell types; including the kidney, heart ventricle, skeletal muscle, skin and sources of cartilage, testis (seminiferous epithelium), ovary, placenta, thymus, prostate, lung, liver, small intestine, pancreas, spleen, colon, blood endothelium and erythrocytes (Sohl, Maxeiner & Willecke, 2005; Zoidl et al., 2007) and in various immune cell lines (Pelegrin and Surprenant, 2006). More recently, Panx1 has been detected in rodent cochlea (supporting cells of the organ of corti, spiral limbus, cochlear lateral wall, strial blood vessels) and in vascular smooth muscle cells (X.-H. Wang, Streeter, Liu, & Zhao, 2009). However, interestingly, regulation of Panx1 expression, mostly in the cortex, cerebellum and eye, has been shown to vary during development. Panx1 shows high expression levels in the embryonic and young postnatal rat brains and levels considerably decline during maturation, at the onset of adulthood (Vogt et al., 2005). Although expression seems to be mainly neuronal (Ray et al., 2005) and localized at postsynaptic sites (Zoidl et al., 2007), Panx1 has still been found in cultured astrocytes and oligodendrocytes (Boassa et al., 2007).

1.2.4 The pannexin channel

Panx1 forms large, low-resistance channels at the plasma membrane that conduct up to 500pS, and allow the bidirectional movement of molecules up to 1.5 kDA; making them permeable to larger molecules like ATP. Recent research has suggested that depending on the stimulation, there is actually a small (50pS) chloride-selective conformation of the channel that exists as well (J. Wang et al., 2014). The gated pores formed by Panx1 connect the intra- and extracellular space, making them reminiscent of Cx hemichannels. Reports show that these channels can be

activated by changes in membrane voltage (hyperpolarization), mechanical stretch, elevated extracellular potassium (K^+) or ATP, elevated cytosolic Ca^{2+} (Pelegrin & Surprenant, 2006), proteolytic cleavage of the Panx1 C-terminal tail at residues 376-379, and following P2 receptor activation (Locovei, Wang, & Dahl, 2006). There is also some evidence to show that certain stimuli can enhance a closed state of the channel; which will be investigated in part in this thesis. The Panx1 channel can also be experimentally manipulated via the use of pharmacological blockers that suppress currents with varying degrees of potency and specificity. Based upon the shared features between Panxs and Cxs, Bruzzone et al (2005) tested the effects of the known Cx blocker on Panx1. For the past 27 years, Carbenoxolone (CBX), a synthetic derivative of BGA – a compound derived from liquorice root, was known to block Cx channels. It was determined that Panx1 responds to CBX at lower concentrations than Cxs, allowing one to differentiate between the activity of the specific proteins during experimentation (Bruzzone, Barbe, Jakob, & Monyer, 2005). The next leading potent compound was determined to be the antimalarial drug mefloquine (MFQ), and disodium 4,4'-diisothiocyanatostilbene-2,2'disulfonate (DIDS), followed by 5-nitro-2-2 benzoic acid, indanyloxyacetic acid 94, probenecid and lastly both flufenamic and niflumic acid were equally found to be poorly sensitive towards blocking Panx1 hemichannels (Ma, Hui, Pelegrin, & Surprenant, 2009). Interestingly, food dye FD&C Blue No.1 (Brilliant Blue FCF [BB FCF]) is also a selective inhibitor of Panx1. It was found to be structurally similar to Brilliant Blue G – a purinergic receptor antagonist, that is a well-known inhibitor of the ionotropic P2X7 receptor (J. Wang, Jackson, & Dahl, 2013). The food dye was found to have a 50% inhibitory concentration (IC_{50}) for concentrations as low as 0.27 µM. This finding is extremely novel and suggests that this 'safe' food dye should be given serious consideration towards pharmacological intervention of Panx1 associated conditions (J. Wang et al., 2013).

1.2.4.1 Trafficking pathway of Panx1

Most of what is understood about Panx1 function comes from cell surface populations; therefore, it is critical to understand the precise signaling mechanisms that regulate anterograde movement to this location. Since Panx1 is an integral membrane protein, its Non-

glycosylated Gly0 core protein is first expressed in the ER where it is glycosylated to Gly1, as mentioned prior. The ER has been proposed to be the region in which oligomerization and Panx interactions occur based upon its important role in the Panx1 life cycle (Peneula et al., 2013). Panx1 then moves to the Golgi via Sar1 dependent COPII vesicles where it becomes the Gly2 species; this occurs in cell types where Panx1 is destined for the cell membrane (Bhalla-Gehi et al., 2010). Cell membrane delivery is untargeted; therefore, Panx1 shows uniform distribution across the membrane (Bhalla-Gehi et al., 2010). There has been some speculation that Panx1 is actually able to remain in part in the ER and intracellularly depending on the cell type, however, this research is yet to be developed. Nonetheless, it is obvious that glycosylation is important for mediating trafficking of Panx1. And by disrupting glycosylation you are actually able to prevent Panx1 membrane expression – Panx1 C-terminal is important for this cell surface trafficking and oligomerization (Gehi, Shao, & Laird, 2011). However, when proper glycosylation occurs and Panx1 makes it to the membrane, it is sequestered in Triton X-100 insoluble lipid rafts, where it remains until it is due for replacement which can be hours or days (Dvoriantchikova, Ivanov, Pestova, & Shestopalov, 2006). Panx1 has been projected to have a very long half-life based upon observations of slow protein displacement and renewal by Boassa et al., (2008) during timed experiments using brefeldin A (BFA) in paired Xenopus oocytes. BFA is used to block protein secretion, which demonstrated a spike in newly synthesized Panx1 localized to the ER, and some cell surface clearing after 32 h, associated with an increase in Gly 1 and a reduction in Gly 2 species respectively (Boassa et al., 2008). This slow turnover rate of Panx1 channels, which is not seen in gap junction proteins, has been proposed to be due to the independence of the microtubule mediated transport (Boassa et al., 2008; Gehi et al., 2011; Penuela et al., 2007). Once Panx1 is due to be removed from the cell surface, it is shuttled to lysosomes for degradation. It is important to note that misfolded or improperly assembled Panx1, which do not have cellular quality control mechanisms, are prematurely degraded via proteasomes. However, the internalization mechanism and the exact mode of degradation, has yet to be elucidated for all Panx1 proteins (Gehi et al., 2011). Trafficking dynamics are likely regulated by the C-terminal domain, where internalization of Panx1 channels is distinct from classical endocytic pathways, but still remain foreign. Although there is

many components of Panx1 trafficking that are left a mystery, it is quite possible that channel activity may be regulated by events that affect channel gating rather than channel assembly and transport.

1.3 Functional Properties of the pannexin1 channel

Panx1 function initiates with the activation of the channel; channel opening. Thus far, research has determined that activation can be achieved via mechanical stimulation (Bao, Locovei, & Dahl, 2004), caspase cleavage (Chekeni et al., 2010), cytoplasmic Ca^{2+}, extracellular ATP and K^{+} (Locovei et al., 2006), and membrane depolarization. In order to abolish the function of Panx1, certain channel blockers can be used such as carbenoxolone, probenecid and fluefenamic acid, as well as mimetic peptides (J. Wang, Ma, Locovei, Keane, & Dahl, 2007). In addition, negative feedback from ATP release can inhibit the channel (Qiu & Dahl, 2009) along with cytoplasmic acidification; which will be investigated in this thesis.

The first functional role of Panx1 originally recognized the protein as a major ATP release channel; four years post its discovery (Bao et al., 2004). Ever since, paracrine functional analysis of Panx1 as an ATP release channel has pioneered cellular biological research; further elucidating other channel functioning properties of Panx1. Our protein of interest has been linked to calcium (Ca2+) signaling, apoptosis and inflammasome responses, sensory adaptation, and it has been shown to contribute to ischemic and epileptic conditions. It is a large plasma membrane channel, therefore, there are many conflicting reports regarding its permeability and protein interactions within the literature. However, with time, functional properties and channel characteristics of Panx1 are slowly becoming decoded and pieced together.

1.3.1 P2 receptors

Certain structural and functional relationships are shared between purinergic receptors and Panx1, allowing the confirmation of various structural and functional roles the protein has on its own and within a dynamic system consisting of the Purinergic P2 receptors (P2X and P2Y). The P2 receptors act as non-selective cation channels that mediate the influx of extracellular Na^{2+} and Ca^{2+}, and the efflux of cytoplasmic K^{+} ions. However, the most important function of the P2

receptors to recognize is that they are well-known receptors for ATP. Seeing as Panx1 is the leading ATP release channel, it is not surprising that there is an established interaction between P2 receptors and Panx1 during physiological and pathophysiological events (Wicki-Stordeur & Swayne, 2014). In 2006, Pelegrin and Suprenant first reported that a large pore, that was permeable to dye, was opened due to P2X7 receptor activation in machrophages. It was later concluded that Panx1 channels were forming the dye permeable pores. In addition, it is understood that P2Xs consist of ionotropic receptors that are linked to ion channels. It was determined that once they became activated, a pore in the membrane was opened and allowed ATP and ions to be released; based upon this, the pore was again concluded to be Panx1 (Coddou, Yan, Osil, Huidobro-Toro & Stojikovic, 2011). MacVicar and Thompson (2010) stated that there was no way P2X7Rs could conduct small molecules on their own, therefore, they must require a secondary ion channel to conduct them for them. As a result, they suggested that Panx1 has to be linked to P2XRs to form a larger pore; allowing the release of ATP, which will be further discussed. There is further compelling evidence to suggest that Panx1 and P2X7Rs interact directly. In heterologous systems, where P2X7 and Panx1 co-express, it was shown that the large pore mediated by P2X7 was actually sensitive to MFQ, CBX and flufenamic acid – much like Panx1. Along with the observed co-immunoprecipitation between Panx1 and P2X7, together, this was enough evidence supporting their direct interaction (R. Iglesias et al., 2008). Additional experimentation confirmed the interaction further, and later began to include P2X4 as a co-precipitant in certain cell types (Hung et al., 2013). Reports vary with regards to the type of interaction experienced between P2 receptors and Panx1. Some agree that P2 receptors are responsible for the activation of Panx1 channels or vice versa (Kanjanamekanant, Luckprom, & Pavasant, 2014; Poornima et al., 2012), some suggest that they associate to form a larger ‘death pore’ (Locovei, Scemes, Qiu, Spray, & Dahl, 2007), others discuss the possibility of them directly forming a complex (R. Iglesias et al., 2008), while others report no influence on the function of each other at all (Weilinger, Tang, & Thompson, 2012). Qu et al (2011) also reported that P2 receptors and Panx1 channels are independent. They used Panx1 KO mouse models to show an increase in membrane permeability when ATP engages P2X7 receptors; suggesting that purinergic receptors and Panx1 proteins are distinct signaling pathways (Qu et

al., 2011). Based upon the different models used, and methods of measuring current, we see a lot of variance in the research. However, there is an overwhelming amount of evidence suggesting that there is some form of interaction present between Panx1 and P2 receptors, which is extremely important for ATP release, immune responses and the mediation of currents; and should always be kept in mind when investigating Panx1 channel functioning.

1.3.2 ATP signaling

ATP serves as a signal for diverse physiological functions; including spreading of Ca^{2+} waves, controlling ciliary beats in airways, and controlling vascular oxygen supply, to name a few. Since, Panx1 is most well-known as the major ATP release channel in a variety of cell types and tissues under both physiological and pathophysiological contexts, it makes the study of the channel mediated ATP release of great importance (Dahl, 2015). The release of ATP was first demonstrated by Bao et al (2004), when they cleverly devised a way to measure reverse potentials from a patch pipette using an ATP gradient set up between the pipette and bath solution (Bao et al., 2004). The efflux of ATP from Panx1 occurs during channel activation, and can also be mediated by ATP itself via ionotropic P2X and metabotropic P2Y purinergic receptors, giving rise to positive ATP feedback loops (Iglesias & Spray, 2012). It is the fact that Panx1 is localized at the post-synaptic membrane that allows the positive or negative feedback at the synapse (Zoidl et al., 2007). Once ATP is released into the extracellular space it allows for the stimulation of more purinergic receptors on the cell itself, and diffuses outward to stimulate other cells nearby; this propagates the ATP mediated ATP release. This feedback loop eventually gets derailed when ATP binds to the extracellular loops of Panx1. Which leads to a reduction in channel conductance, ultimately preventing further effects from ATP; both the permeability and release of it (Iglesias & Spray, 2012). This discovery led to observing the application of ATP in aiding intercellular Ca^{2+} signaling, which will be discussed later. ATP also can act as a danger signal, as Locovei et al (2007) found that oocytes undergo apoptosis when exposed to large amounts of the molecule, which tends to be released from the cell under times of threat. This indicates that Panx1 channels must be remaining open for extended periods of time during such conditions. Overall, it is apparent that ATP has the ability to govern

indirect communication between cells, which can indicate paracrine signaling functions of Panx1 (Bennett & Zukin, 2004).

1.3.3 Calcium Waves

The initiation of intracellular Ca^{2+} release from ER stores occurs when extracellular ATP increases and binds to purinergic receptors, allowing the increase in inositol 1,4,5-triphosphate (IP_3) and its associated Ca^{2+} release (Berridge, Bootman, & Roderick, 2003). Upon intracellular Ca^{2+} levels increasing, it facilitates Panx1 channel opening in cells allowing the release of ATP, which acts as the diffusible agent that mediates the spread of focally raised levels of Ca^{2+} between cells that are not in physical contact. A positive feedback occurs between Ca^{2+} and ATP, once Ca^{2+} activates single-membrane channels, further releasing ATP and in turn playing a key role in intracellular Ca^{2+} propagation to neighbouring cells. Pelegrin and Surprenant (2006) are strong believers in Panx1 playing an integral part in the Ca^{2+} signaling, based upon their main function as ATP release channels and the fact that they are key interacting partners with P2XRs. Alternatively, Locovei et al (2007), deems Panx1 as a player in the initiation and propagation of regenerative Ca^{2+} signaling via P2YR interactions. In addition, Kurtenbach et al (2013) conducted dye uptake experiments in cell culture providing compelling evidence of Panx1 acting as a Ca^{2+} signaling sensitive channel; showing increase in dye uptake under increased levels of intracellular Ca^{2+} (10μM) (Figure 5). Therefore, Panx1 can be identified as a mediator of initiating and propagating regenerative Ca^{2+} waves for long-range communication, suggesting another role in paracrine signaling for Panx1. However, issues arise when we consider how large a role gap junctions play in direct cell- to-cell communication. If the right model or method is not used, Ca^{2+} propagation could be easily confused as primarily a Panx1 or a Cx function, though; it is likely a mechanism that occurs in unison.

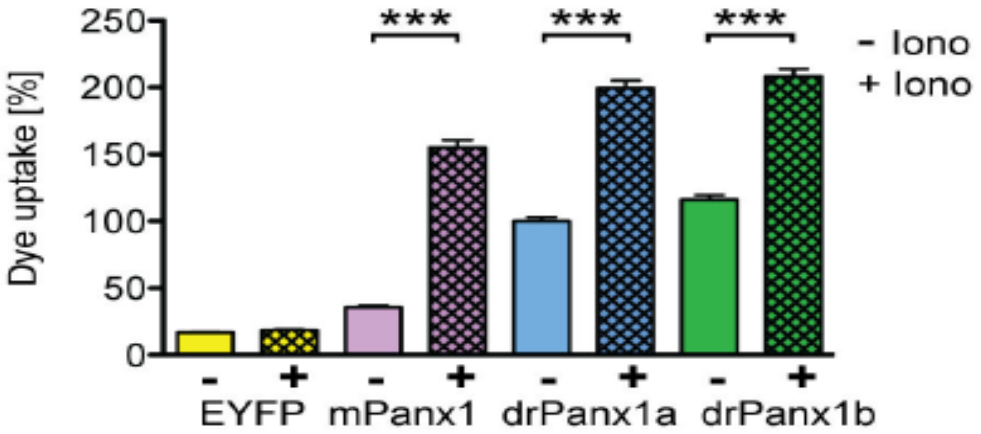

Figure 5: Calcium stimulated Panx1 dye uptake assay confirming the role Panx1 plays in calcium signaling. Ionomycin (Iono) was used to raise intracellular Ca2+ levels in order to stimulate Ethidium bromide (EtBr) dye uptake in cells expressing various Panx1 homologs. Upon increased intracellular Ca2+ we can see increased dye uptake, suggesting that the Panx1 channel is opening and may be responsible for the ATP release that aids in Ca2+ wave propagation. Figure adapted from PLOSone (Kurtenbach et al., 2013).

1.3.4 Inflamasomme, apoptosis and viral responses

Numerous studies have indicated that Panx1 holds various roles in the innate immune system. In 2006, Dahl and Locovei indicated that Panx1 and P2XRs together function in the inflamasome complex. Inflamasomes, being molecular platforms, are activated during cellular infection or stress; resulting in the maturation of pro-inflammatory cytokines like interleukin-1B that activate innate immune defenses (Schroder & Tschopp, 2010). Dahl and Locovei (2006) propose that it is the ATP released from the Inflamasome response that stimulates ionotropic P2XRs to interact with Panx1, and ultimately activate caspase-1 and subsequent pro-inflammatory cytokine release. Meanwhile, in macrophages, it is suggested that once P2XRs are activated by extracellular ATP, it leads to Panx1 channels opening, thereby enhancing ATP release, and initiating downstream innate immune system responses (Pelegrin & Surprenant, 2006). The interaction between Panx1 and ionotropic $P2X_7$ receptors has also been shown to regulate specific cell death signaling. In *Xenopus* oocytes, only Panx1 and $P2X_7R$ co-expression led to ATP induced zeiosis, suggesting that these proteins form a 'death complex.' Otherwise, Panx1 channels have been proposed to release 'find me' signals during apoptosis. During times of

stress, Panx1 channels are activated and cleaved by caspases, which allow further ATP release. This nucleotide release acts as the signal from apoptotic cells to attract phagocytes (Chekeni et al., 2010). Although there exists some conflicting evidence with the understanding of Panx1's role in the immune response (Séror et al., 2011), it has been established that ATP release via Panx1 plays an important role. As mentioned above, it is the understanding that IL-1β is released and in turn caspase-1 is activated due to the efflux of ATP from Panx1. In neuronal and astrocytic inflamasomes, this response is suggested to be potentiated by high extracellular K^+ levels that occur during cellular stress – for example, events like epileptic seizures. Immune responses via Panx1 have been proposed to be otherwise based upon Toll-like receptor-independent inflamasomes, triggered by Panx1 itself (Séror et al., 2011).

Panx1 has also been identified as being part of the infection synapse orchestrated by a virus in order to facilitate infection of $CD4^+$ cells (Séror et al., 2011). During infection, ATP is released from Panx1 channels once HIV-1 envelope proteins interact with the receptors on $CD4^+$ cells. ATP then acts on P2Y2 receptors to activate Pyk2 kinase, which results in membrane depolarization. This then facilitates membrane-membrane fusion and then cell-to-cell transmission, allowing the entry of the virus into the cell. Research suggests that viral replication or HIV-1 infection, can be impaired by blocking or inhibiting any of the components in this 'infection synapse;' making Panx1 in particular a likely target for novel antiretroviral therapy (Séror et al., 2011).

There is compelling evidence for the role of Panx1 in apoptosis as well as the inflamasome and viral responses. However, KO mouse studies have given reason to believe that Panx1 is not required for inflamasome activation, although suggesting that they do maintain a key role in the release of chemoattractants for phagocytic cells to induce appropriate apoptotic cell clearance (Qu et al., 2011). Taken together, there is a wealth of reason to believe that Panx1 does have a dynamic role in the complex innate immune response, but more research is still required at this time.

1.3.5 pH sensitivity

Kurtenbach and colleagues, in 2013, determined that Panx1 functioned as a pH dependent channel. They controlled the pH of the extracellular environment of Neuro2a cells transfected with Panx1a, 1b and mouse Panx1, and tested for the cellular uptake of Ethidium Bromide (EtBr). Each homolog demonstrated the same response to changing environmental pH; when one decreases the level of pH, the amount of dye uptake decreases. Conversely, when the level of pH in the extracellular space increases, the amount of dye uptake increases as well. It is important to note that there is some dye uptake at the physiological pH range as well (Figure 6). This suggests that under pathophysiological conditions when the CNS experiences acidification (decreased pH) or alkalization (increased pH), the Panx1 channels are closing and opening respectively. This gating property can have serious biological effects on the functioning of the cell and its interactions, since maintaining Panx1 channel opening for extended periods of time could be detrimental to internal ATP and glucose stores. The study of pH dependence goes beyond diseased models, as it is understood that the physiological modification of pH is related to critical processes such as development, neuronal activity, lateral inhibition in the outer retina and the circadian clock (Kurtenbach et al., 2013). It is obvious that the mechanistic gating properties of Panx1 need to be elucidated to shed some light on both the functionality of the protein physiologically, and the consequences of the dysfunction of the protein pathophysiologically. As a result, this channel-gated sensitivity to pH will be investigated in further detail in this thesis.

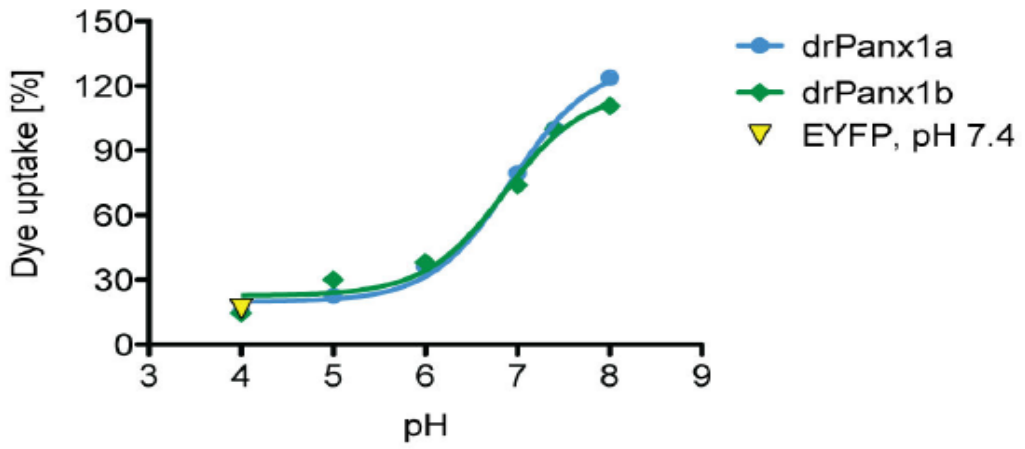

Figure 6: Analysis of the influence of extracellular pH levels on dye (EtBr) uptake in drPanx1 transfected N2a cells. drPanx1a is indicated in blue, and drPanx1b is shown in green, EYFP control is indicated by the yellow arrow. Panx1 hemichannel pH dependent activity demonstrated by manipulating extracellular pH levels. The channel uptakes more dye when the pH levels increase and abolishes dye uptake when the pH level decreases. Figure adapted from PLOSone (Kurtenbach et al., 2013).

1.4 Physiological and pathophysiological relevance of Pannexin1

The physiological relevance of Panx1 has been quite difficult to elucidate based upon the fact that it is such a large pore that typically is found to remain open, which is likely to kill neurons (Kapur, 2012). In fact, under many pathophysiological conditions, the pore remains open for extended periods of time; this will be investigated in this thesis with regards to both ischemic and epileptic environments. There exists many experimental methods that use pharmacological agents, over-expression studies, RNA interface, and mouse knockout lines, in order to modulate Panx1 function and decipher its physiological role. Thus far, knockout studies have determined that abolishing the Panx1 protein altogether results in certain behavioural, learning and memory abnormalities (Kurtenbach et al., 2014). However, there is also therapeutic evidence for blocking Panx1 during epileptic seizures (Santiago, Veliskova, Patel, Lutz, Caille, Charollais, Meda, Scemes, et al., 2011). Therefore, although there is much left to learn about the gating properties of Panx1 at a cellular level, there is still much emphasis on gaining an understanding of its patho- and physiological importance at a systems level as well.

1.4.1 Sensory adaptation

ATP is a key player in sensory adaptation, as a result, Panx1 has been implicated in the processing of various senses (Dando & Roper, 2009). Research has sought to determine the potential role Panx1 could play in the various sensory systems; including but not limited to processing taste, audio, visual and olfactory stimuli. The presence of Panx1 has been determined in these different chemosensory systems, thus, raising the general question of whether Panx1 may contribute to sensory perception via ATP release – modulating purinergic signaling (Kurtenbach et al., 2013). For instance, in taste buds there are two types of cells; one being the receptor cells that express taste receptors. Activation of these receptors on the post-synaptic cell elicits ATP release, and in turn, causes the stimulation of purinergic receptors on the presynaptic cell to induce neurotransmitter release (serotonin) into the synapse. It is this cell-cell signaling that provides the means for information processing within the taste bud (Huang et al., 2007). ATP has also been found in other situations where it is likely responsible for the perception of sensory stimuli. For example, in the retina, purinergic signals act as neuro- and glio-transmitters where they likely modulate retinal responses (Prochnow et al., 2009). In the cochlea ATP can modulate sensitivity of hearing, sound transduction, neurotransmission, and also influences gap-junctional coupling (Zhu & Zhao, 2012). Based upon the fact that Panx1 has been reported to be expressed in these systems, and ATP clearly has a functional role, taken together, the research suggests that Panx1 is responsible for mediating the ATP release that modulates sensory processing (Murata et al., 2010).

1.4.2 Olfactory system

During evolution, the olfactory system has developed the ability to detect and discriminate between odours in order to communicate, forage, mate and avoid predators or foul nutrition (Chuah & Zheng, 1992). In order to accomplish this, vertebrates require a highly organized olfactory system, which with time, has developed to detect a vast amount of volatile chemicals. In humans there is only one functional structure required for olfaction, known as the main olfactory epithelium; this is present in rodents as well. However, rodents have also developed several subsystems that aid in increasing the complexity of the olfactory system; resulting in the

ability to detect higher orders of odour discrimination. This increased complexity of the olfactory system is essential for lower vertebrates because they do not possess the same degree of development or sensitivity in their other sensory systems, like the trichromatic colour visual system in humans. Other olfactory subunits present in mammals, excluding humans, include the Grueneberg ganglion (GG), vomeronasal organ (VNO), septal organ (SO), and accessory olfactory bulb (AOB) (Figure 7). In brief, the GG is a compartment populated with ciliated neuronal cells that may operate as a dual sensory organ involved in the detection of both chemical and thermal stimuli (Fleischer & Breer, 2010). While the SO is a distinct chemosensory organ with axons that project and fasciculate into several discrete bundles that terminate in a subset of the main olfactory bulb, likely specialized for early detection of biologically relevant odorants. However, it is still unknown if these cells are functionally responsive to odorants (Storan & Key, 2006). The VNO, is a sensory organ that contains pseudostratified neuroepithelium that mediates pheromone detection to initiate behavioural responses, and the AOB is where many of the sensory neurons from the VNO synapse (Pérez-Gómez, Stein, Leinders-Zufall, & Chamero, 2014). The epithelial segregations present for processing chemosensory information in the AOB are known to exist in most mammals, however, the information each processes are widely unknown.

Native to all mammals alike, are the three main cell layers present in the main olfactory epithelium (OE). These include the sustentacular or supporting cell layer – which is responsible for metabolic and physical support of the olfactory cells, the olfactory neuron layer and the basal cell layer, which differentiates into either supporting or olfactory cells; and is responsible for total replacement of the OE every 2-4 weeks (Mombaerts 2004). The OE is always in contact with inhaled air, where the odorants come in contact with the mucus layer that contains the supporting cells and bind to odorant binding proteins in order to reach the cilia of the olfactory neurons; where they either directly dissolve or bind onto receptors on the cilia of the olfactory sensory neurons (OSNs) (Figure 7). This event then elicits a signal transduction cascade involving adenosine triphosphate (ATP) and its ability to elicit increases in intracellular Ca^{2+}, which goes through the axons of the OSNs and converge into glomeruli in the olfactory bulb, which then continues to be processed in higher brain regions (Kurtenbach et al., 2014).

The VNO has both an apical and basal region that each project to, and synapse in, different areas of the AOB for further processing. Current analysis has shown that each region of the VNO is responsible for processing different odorants, however, it is largely unclear what each region is responsible for. Thus far, researchers have used chemosensory ligands to reveal that the fundamental role of the basal region is to mediate a wide range of instinctive behaviours like aggression, predatory avoidance and sexual attraction (Perez-Gomez et al., 2014). Unlike other sensory systems that are developed to encode a single parameter, like wavelength or frequency, the olfactory system had to evolve a complex network capable of detecting and discriminating the structurally and chemically heterogeneous class of volatiles, molecules and odours.

Several Cxs are expressed in the OE and have demonstrated the ability to modulate olfactory sensitivity by electrically coupling OSNs, although precise function is still unclear (Zhang, 2011). It is also understood that ATP modulates olfactory responsiveness and in turn plays a role in proliferation, differentiation and regeneration of OSNs. ATP is also released from the vomeronasal organ (VNO) during mechanical stimulation where it elicits intracellular Ca^{2+} and reduces the responsiveness of OSNs to odorants (Vick & Delay, 2012). Since both Panx1 and purinergic receptor expression has been confirmed in various locations of the olfactory system, it is fair to believe that Panx1 may play a part in the paradoxical world of olfactory processing.

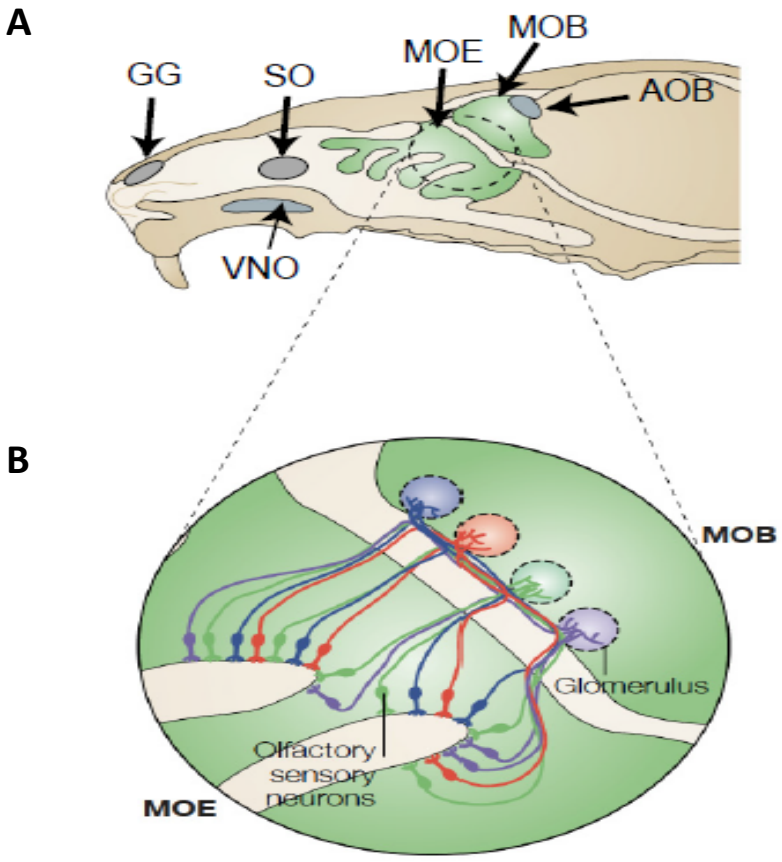

Figure 7: Simplified overview of the mammalian olfactory system. A) Demonstrates the location of the main olfactory epithelium (MOE) and the main olfactory bulb (MOB) in green, and neurons in the vomeronasal organ (VNO) projecting to the accessory olfactory bulb (AOB) – both highlighted B) Shows the projection of olfactory sensory neurons (OSNs) to the MOB, where OSNs expressing the same olfactory receptor, project to the same glomerulus, indicated by colour. Figure modified and adapted from Nature Reviews Neuroscience (Mombaerts, 2004).

1.4.3 Ischemia

The first indication that Panx1 could be involved in pathology occurred in 2006 when Thompson et al proposed that the massive disruption in electrochemical gradients, seen across plasma membranes in hippocampal neurons when challenged by oxygen (O_2) and glucose deprivation, could be the result of Panx1 channel activity. This idea flourished when experiments using CBX

and dye transfers strongly supported the idea that Panx1 was involved. Others have since persisted to show that during oxygen/glucose deprivation (OGD), which occurs when there is reduced blood supply to the cells – initiating necrotic cell death due to a surge of ions and neurotransmitters like glutamate, blocking or knocking out Panx1 shows significantly less damage suffered (Dvoriantchikova et al., 2012). A large body of evidence in the past has shown that prolonged OGD and ischemia can lead to damage due to the opening of Panx1 (Kapur, 2012). It is suggested that Panx1 channel opening can occur due to the release of glutamate upon OGD binds to NMDARs to activate Panx1. As a result, this opening can be responsible for anoxic depolarization of pyramidal neurons that occurs during stroke, and/or the excitotoxicity that results in cell death during ischemia (Weilinger et al., 2012). There is also evidence suggesting that the mitochondrial pathway senses the reduced O_2 during such conditions, eliciting Panx1 mediated ATP and Ca^{2+} release from neurons, and the display of inward currents; leading to mitochondrial depolarization, oxidative stress and resulting in cell death (Iwabuchi & Kawahara, 2011). This oxidative stress that results from OGD is something of interest to the devotees of Panx1 research. The oxidative stress leads to a shift in the extracellular pH, which is shown to be a factor in controlling Panx1 gating; this will be expanded within this thesis. To further support the role Panx1 plays in ischemia, studies on cerebral ischemia were conducted to show that double KO mice (both Panx1 and 2) had a significant effect on the function of cortical neurons; showing smaller infarcts during ischemic stroke and potential for therapeutic targeting (Bargiotas et al., 2011).

1.4.4 Epilepsy

MacVicar and Dudek in 1980 first suggested that electrotonic junctions could be an important factor in generating epileptiform activity. Tracing back to when the trending notion was 'Panx1 was a gap junction,' it was speculated that Panx1 contributed to seizure like events as well. Many years later, Panx1 was found to show expression at postsynaptic sites In CA1 pyramidal neurons in the hippocampus, where NMDA receptors were shown to participate in the activation of secondary currents. As a result, Thompson et al (2008) tested the interaction between Panx1 and NMDA receptors, to investigate their role in epilepsy. They showed that by

triggering prolonged epileptiform activity, by removing external magnesium ions (Mg^{2+}), it enhanced the activation of NMDARs, while decreasing spike amplitude and burst intervals during the application of Panx1 blocking peptides. They concluded that not only can Panx1 opening be activated by NMDAR stimulation, but also this channel protein can contribute to epileptiform seizure activity (Thompson et al., 2008).

Knockout mouse models have been used to demonstrate that Panx1 channels contribute to status epilepticus *in vivo* by increasing the severity and duration of seizures. This data is in line with reports of Panx1 interacting with NMDA receptors in hippocampal pyramidal neurons showing their participation in the regulation of Ca^{2+}, which is suspected to potentiate seizure like activity (Thompson et al., 2008). In human models, there has been elevated Panx1 expression levels detected in the temporal lobe cortex of patients with temporal lobe epilepsy, which were determined using standard western blotting techniques (Jiang et al., 2013). This likely suggests that Panx1 channels are important in the formation of epilepsy; however, this remains to be further investigated.

During epileptic convulsions, intense neuronal hyperactivity can induce the elevation of extracellular K^+ to levels that can promote Panx1 channel opening (Santiago, Veliskova, Patel, Lutz, Caille, Charollais, Meda, & Scemes, 2011). Therefore, it was hypothesized that once Panx1 is stimulated, for example with K^+, it is responsible for releasing a surge of ATP that contributes to the manifestations of seizures. The ATP is metabolized via ecto-nuleotidases into adenosine, which can inhibit presynaptic neurotransmitter release and act as an anticonvulsant (Carlen, 2012). This was tested via both knockout mice and cellular models, including ATP release and dye uptake assays, and both methods yielded the same results. It was concluded that Panx1 channels do not participate in the onset of seizures, but are activated during *in vivo* neuronal hyperactivity. In addition, they contribute to non-vesicular ATP release, which is thought to activate purinergic receptors, and substantially contribute to increasing and prolonging the duration of seizure activity (Santiago et al., 2011). Therefore, taken together, there are clearly beneficial effects seen in Panx1 null models. This is possibly due to the prevention of losing

cellular ATP stores, which impairs post epileptic recovery from prolonged seizures, suggesting that Panx1 is a novel target for therapeutic approaches.

Research conducted with Panx1 in an ischemic environment naturally led to correlating Panx1 with epileptic events as well. Seeing as Panx1 induces depolarization and cellular excitability during a stroke, it was only logical to presume that it was responsible also for fuelling the deregulated neuronal activity experienced during an epileptic seizure. There have been many challenges in understanding the role of Panx1 channels in seizures and epilepsy, based upon the fact that there is a lack of specific drugs and ways to inhibit the channel; many drugs can activate and inhibit these channels but they often can have off target effects (Santiago et al., 2011). Regardless, there is no doubt that Panx1 channels are related to epilepsy, and now with the development of transgenic mice, this relationship is undeniable. However, there is a great deal of information regarding how Panx1 plays its part in epileptic events that have yet to be uncovered.

1.5 Motivation, objectives and highlights

Panx1 is coined as the major ATP release channel within vertebrates, deeming Panx1 a foreseeable participant in paracrine signaling. In addition, ATP is understood to modulate chemosensory function. As a result, it is of great interest to investigate the gating mechanism responsible for the efflux of ATP from Panx1 during physiological and pathological conditions. Preliminary work performed on the mouse neuroblastoma cell line, Neuro2A (N2A, ATCC), demonstrated that it is possible to retrieve reliable baseline recordings of ATP release using a luciferase based assay technique (Appendix H). Various modes of stimulation were tested in cell culture, and shifted to a knockout mouse model in order to develop an understanding of how ATP release occurs *in vivo.* Other researchers used KO mouse models to determine that Panx1 mediates ATP release from airway epithelia and showed compromised channel functioning, which made studying Panx1 function in the olfactory system relevant. The objective of conducting ATP detection assays in the olfactory system of KO mice was to elucidate the role that Panx1 plays in olfaction itself, seeing as there is strong evidence supporting Panx1's role in other sensory systems like in taste buds and the retina, see chapter 4. In this study, the impact

of Panx1 ablation in the olfactory system was characterized and Panx1 localization was determined. Taken together, it was tempting to hypothesize that Panx1 mediates the ATP release responsible for modulating OE and VNO function, however, results suggested a different role than anticipated.

Further work conducted in chapter 5 was inspired by research piloted by Kurtenbach et al, (2013), which exploited the sensitivity of Panx1 channels to pH by manipulating the pH levels of extracellular solutions. These results suggested that Panx1 channels close during acidification, a phenomenon that occurs during ischemia, and open upon alkalinisation, a staple of epileptic environments. However, to date it has been understood that under experimental ischemic conditions, Panx1 channels actually remain open to allow an efflux of ATP. Interestingly, the loss of ATP under these conditions, and the activation of a cell death pathway – not investigated in this study, can lead to neuronal cell death. Meanwhile, it is perplexing as to why, during basic conditions, channel functions seem to align with the environmental conditions. Here, with the use of live cell dye uptake assays, the objective was to isolate the region of Panx1 that is responsible for modulating pH sensitive channel gating in order elucidate this puzzle. If successful, it is hoped that this research will identify a potential target for manually controlling Panx1 hemichannel activity during pathological situations for therapeutic attainment.

Based upon all of the physiological and pathophysiological contexts that Panx1 acts within, it further highlights and supports the importance of determining precise regulation of Panx1 channel gating properties and studying the channel from a translational research perspective. Ultimately, hoping to provide a platform for developing therapeutic targets and the means towards illustrating definitive mechanistic and structural properties of the protein.

2. Materials

"Scientific work must not be considered from the point of view of the direct usefulness of it. It must be done for itself, for the beauty of science, and then there is always the chance that a scientific discovery may become like the radium, a benefit."

- Marie Curie

2.1 Firm index

All companies and their headquarters are listed in the appendix A Firm index.

2.2 Biosaftey

The research projects completed in this thesis were performed in accordance with federal, provincial and institutional regulations for the containment Level 2 laboratories located at the Life Science Building (LSB), Department of Biology at York University.

2.3 Organisms

Handling, manipulation and storage of all recombinant bacterial or eukaryotic cell lines was performed in licensed S2 laboratories located at the Department of Biology at York University, Toronto Ontario. The breeding and handling of mice was permitted by Animal Care Committee (York University, Canada).

2.3.1 Bacterial strain

Escherichia coli (*E.coli*) DH5α (Invitrogen, Burlington, Canada)

Genotype: F^- Φ80*lac*ZΔM15 Δ(*lac*ZYA-*arg*F) U169 *rec*A1 *end*A1 *hsd*R17 (r_k^-, m_k^+) *pho*A *sup*E44 *thi*-1 *gyr*A96 *rel*A1 λ^-

E.coli NEB 5-alpha competent (New England Biolabs, Whitby, Canada)

Genotype: *fhuA2 Δ(argF-lacZ)U169 phoA glnV44 Φ80 Δ(lacZ)M15 gyrA96 recA1 relA1 endA1 thi-1 hsdR17*

2.3.2 Eukaryotic cells

Neuroblastoma 2a cells (Neuro 2a or N2a cells) were derived from *Mus musculus.* Klebe and Ruddle developed this cell line in 1967 from a spontaneous tumour of a strain A albino mouse (Klebe and Ruddle, 1969). The N2a cells were kindly provided by Prof. David C. Spray (Albert Einstein College, NY, USA).

2.3.3 Animals

Panx1 wildtype (+/+) (WT) and knockout (-/-) (KO) mice

Handling and housing of animals used to complete this thesis was performed in compliance with the German Animal Rights law and had formal approval by the Animal Care Committee (York University, Canada). Animals were housed with a 12-hour light/dark cycle and had free access to food and water. Male mice were housed individually 1 week prior to use and were 4-8 months of age prior to use. The generation of $Panx1^{+/+}$ mice (Panx1fl/fl) with three LoxP consensus sequences integrated into the Panx1 gene, flanking exon 3-4, and knockout mice with global loss of Panx1 ($Panx1^{-/-}$, CMV-Cre/Panx1), were described previously (Dvoriantchikova et al., 2012) and provided to our lab by Dr.Valery Shestopalov from the Bascom Palmer Eye Institute at the University of Miami. Although Panx1 expression in tissues is ubiquitous, no major abnormalities in the anatomy or overall health of Panx1 KO mice are reported.

2.4 Chemicals

Table 1: List of chemicals.

Chemical	Company	Chemical	Company	Chemical	Company
Acetic Acid Glacial	Bioshop	Formaldehyde solution (Formalin)	Sigma	Odyssey blocking buffer	LI-COR Biosciences
Acrylamide	Bioshop	Glucose	Fisher	Orange G	Invitrogn
Agar	Bioshop	L-glutamine (100X)	Life technologies	Potassium Chloride	Sigma
Agarose	Fisher	Glycerol	Bioshop	Potassium gluconate	Sigma
Ammonium persulphate (APS)	Bioshop	Glycine	Bioshop	Sodium Chloride	Sigma
Bacto tryptone	Fisher	LB-Agar-Pulver	AppliChem	Sodium dodecyl sulphate	Bioshop
Bromphenol Blue	Bioshop	LB-Medium-Pulver	AppliChem	Tetramethylethylene-diamine (TEMED)	Bioshop
Bovine serum albumin (BSA)	PAA	N-2-hydroxyethyl piperazin-N-2-ethanesulfonic acid (HEPES)	Sigma	Tris(hydroxymethyl)	Sigma
Calcium Chloride	Bioshop	Immersion oil	Zeiss	Triton X-100	Sigma
Ethylenediaminetetraacetic acid (EDTA)	Bioshop	Isopropanol	Bioshop	Trypsin-EDTA	Sigma
Ethanol	Commercial ALC	Magnesium chloride	Fisher	Tween 20	AppliChem
Ethidium Bromide	BioShop	Non-essential amino acids (100X)	Thermo Fisher Scientif	Water (ultraPURE Distilled Water DNAse RNAse free)	Invitrogen
Fetal bovine serum (FBS)	Life technologies	Normal Goat Serum (NGS)	Biotech	Xylene Cyanol FF	Bioshop

2.5 Antibiotics

Kanamycin was purchased from BioShop

2.6 Antibodies

Table 2: Description of the primary antibodies used for completion of western blots for pH sensing experimentation with Panx1a and the associated alanine and histidine mutations.

Name	Species of Origin	Source	Dilutions
anti-GFP (Poly)	Rabbit	Santa Cruz	1 to 200
anti-β-actin	Mouse	Sigma-Aldrich	1 to 3 000

Table 3: Description of the secondary antibodies used for completion of western blots for pH sensing experimentation with Panx1a and the associated alanine and histidine mutations.

Name	Species of Origin	Source	Dilutions
anti-mouse iRDye (Poly) 800	Goat	Li-Cor	1 to 2 000
anti-rabbit iRDye (Poly) 680	Donkey	Li-Cor	1 to 3 000

2.7 Enzymes

Q5® Hot Start High-Fidelity 2x Master Mix; 10x KLD enzyme mix, Phusion High-Fidelity DNA Polymerase, FastDigest restriction endonucleases, T4 DNA ligase All enzymes were purchased from New England BioLabs.

2.8 Kits

Table 4: List of kits utilized for various applications in the laboratory.

Procedure	Kit name	Company name
Site directed mutagenesis	Q5® Site-Directed Mutagenesis Kit	New England BioLabs
Plasmid DNA Purification	QIA Prep Spin Miniprep Kit	QiaGen
ATP determination	Molecular Probes® ATP Determination Kit	Life Technologies
Immunodetection	iBind™ Western Systems	Life Technologies
DNA transfection	Effectene Transfection Reagent	QiaGen
Polymerase Chain Reaction (PCR)	Phusion High Fidelity PCR Kit	Thermo Scientific
Purification of PCR and DNA fragments	NucleoSpin® Gel and PCR Cleanup Kit	Clontech
iBIND Western Blot	iBind™ Solution Kit	Life technologies

2.9 Plasmids and Oligonucleotides

2.9.1 Phylogenetic Analysis of plasmid

The drPanx1a coding sequence was downloaded from a protein query, and then the nucleotides were focused on to retrieve the mRNA sequence, from the National Center for Biotechnology Information (NCBI) database (Table 5).

Table 5: Pannexin protein sequence accession gathered from NCBI. Used for phylogenetic analysis and further processing for mutagenic experimentation.

Species	Protein	Accession
D. rerio (zebrafish)	Panx1a	NM_200916 XM_697309

Table 6: List of used commercially available plasmids.

Plasmid name	Description	Source
pEYFP	eukaryotic expression vector encoding for fusion proteins consisting of the N-terminal protein of interest with a C-terminal EYFP-tag, kanamycin resistance	Clontech

Table 7: List of plasmid constructs generated by site-directed mutagenesis.

Vector	Insert	Description of Usage
pEYFP-N1	drPanx1a	Analyses of C-terminal EYFP-tagged Panx1 gating properties using pH adjusted medium and fluorescent dye uptake analysis
	drPanx1a ΔP98A	" "
	drPanx1a ΔW100A	" "
	drPanx1a L101A	" "
	drPanx1a H102A	" "
	drPanx1a K103A	" "
	drPanx1a W100H/H102A	" "
	drPanx1a L101H/H102A	" "
	drPanx1a K103H/H102A	" "
	drPanx1a F104H/H102A	" "
	drPanx1a F105H/H102A	" "

2.9.2 Oligonucleotides

Table 8: List of oligonucleotides. Primers designed from NEBase changer and used in PCR for site directed mutagenesis to complete experimentation on pH sensing of the Panx1a protein. TM indicates the annealing temperature. Bolded letters indicate the mutated nucleotides to alanine, single underline indicates the mutation H102A, double underline indicates the nucleotides mutated to histidine.

Target	Primer Sequence	TM (°C)	Size (bp)
Panx1a: P98A	F: 5'-TGGAGGCCTT**GCT**TTATGGCTGC -3' R: 5'-GTGTCCTGTTTCTGCACTGC -3'	67°C	23 20
Panx1a: W100A	F: 5'-CCTTCCTTTA**GCG**CTGCATAAGTTTTTCCC -3' R: 5'-CCTCCAGTGTCCTGTTTC-3'	59°C	30 18
Panx1a: L101A	F: 5'-TCCTTTATGG**GCG**CATAAGTTTTTCCCTTATATC -3' R: 5'-AGGCCTCCAGTGTCCTGT -3'	65°C	35 18
Panx1a: H102A	F: 5'-TTTATGGCTG**GCG**AAGTTTTTCCCTTATATCCTGCTGCTG -3' R: 5'-GGAAGGCCTCCAGTGTCC-3'	64°C	37 18

Panx1a: K103A	F: 5’-ATGGCTGCAT**GCT**TTTTTCCCTTATATCCTGC -3’ R: 5’-AAAGGAAGGCCTCCAGTG -3’	61°C	32 18
Panx1a: W100H/H102A	F: 5’- CCTTCCTTACATCTGGCTAAGTTTTTCCC-3’ R: 5’-CCTCCAGTGCCTGTTTC-3’	58°C	30 18
Panx1a: L101H/H102A	F: 5’-TCCTTTATGGCATGCTAAGGTTTTCCCTTATATC-3’ R: 5’-AGGCCTCCAGTGTCCTGT-3’	64°C	34 18
Panx1a: K103H/H102A	F: 5’- ATGGCTGGCTCATTTTTTCCCTTATATC-3’ R: 5’-AAAGGAAGGCCTCCAGTG-3’	61°C	28 18
Panx1a: F104H/H102A	F: 5’- GCTGGCTAAGCATTTCCCTTATATCC-3’ R: 5’-CATAAAGGAAGGCCTCCAG-3’	61°C	26 19
Panx1a: F105H/H102A	F: 5’- GGCTAAGTTTCATCCTTATATCCTGCTG-3’ R: 5’-AGCCATAAAGGAAGGCCTC-3’	61°C	28 19

2.10 Size standards

2.10.1 DNA size standards

GeneRuler 1Kb Plus DNA Ladder Fermentas

2.10.2 Protein size standards

PageRuler Plus Prestained Protein Ladder Fermentas

2.11 Media and Solutions

2.11.1 Solutions and media for cell culture

Table 9: solutions used for cell culture, including company of retrieval.

Solutions	Company of Retrieval
10% Formalin	Sigma-Aldrich
Trypsin-EDTA solution	Sigma-Aldrich
PBS -/- (no Ca^{2+} or Mg^{2+})+/Mg2+	Sigma-Aldrich
PBS +/+ (0.0133% calcium chloride dehydrate & 0.01% magnesium chloride hexahydrate)	Sigma-Aldrich
Penicillin and Streptomycin	BioShop
FBS (Fetal Bovine Serum)	Gibco
NEA (Non-essential Amino Acids)	Sigma-Aldrich
Dulbecco's Modified Eagle Medium (DMEM)	Sigma-Aldrich
Mounting Solution: Fluoroshield with DAPI	Sigma-Aldrich

Note: composition of growth media for N2a cells: DMEM (4.5 g/l D-glucose, +L-glutamine, -pyruvate) + 10% FBS, 1% L-glutamine, 1% NEA,1% penicillin/streptomycin (10,000 U/ml/10mg/ml), 1mM Na-pyruvate, used both with and without phenol red – which had additional +1% L-glutamine supplemented.
Composition of Trypsin: 0.05% trypsin, 0.02% EDTA (1x) in D-PBS (PAA)
Composition of PBS: 130mM NaCl, 2.8 mM KCl, 10mM Na_2HPO_4

Table 10: solutions used for stable and transient transfection of cell culture, including company of retrieval.

Solutions	Company of Retrieval
Effectene®	QiaGen
EC Buffer	QiaGen
Enhancer	QiaGen
Dulbecco's Modified Eagle Medium (DMEM)	Sigma-Aldrich
G418	Sigma-Aldrich

2.11.2 Solutions and media for cultivation of bacteria

Table 11: Solutions and media used for cultivating bacteria. Solutions were used for the transformation of plasmid DNA.

Solution and Media	Composition
LB Media	1% baco trytone, 0.5% yeast extract, 0.5% NaCl, 50 µg/mL of kanamycin
LB Agar plates	LB medium (+1% agar), 50 µg/ml of Kanamycin
SOC Medium	2% bacto typtone, 0.5% bacto yeast extract, 10mM NaCl, 2.5 mM KCl, 10 mM $MgCl_2$, 10mM $MgSO_4$, 20mM glucose

2.11.3 Solutions and media for molecular biology

Table 12: Solutions for molecular biology.

Solution	Composition
6x DNA Loading Buffer	10 mM Tris-HCl (pH 7.6), 0.03% bromophenol blue, 0.03% xylene cyanol FF, 60% glycerol, 60 mM EDTA, (Fermentas)
1x Tris-acetate-EDTA (TAE) Gel Loading Buffer	40mM Tris, 20mM acetic acid, 1mM EDTA

2.11.4 Solutions and media for protein biochemistry

Table 13: Solutions used for Protein Biochemistry – Western Blotting analysis.

Solution	Composition
Laemmli Sample Buffer	2% SDS, 10% glycerol, 5% β-mercaptoethanol, 0.1% Orange G, 50 mM Tris-HCl: pH 6.8
Laemmli Running Buffer	192mM glycine, 0.1% SDS, 25 mM Tris-HCl: pH 8.3
Staining Solution	Coomassie PAGE BLUE (BioRad)
Blocking Solution	Odyssey Blocking Buffer (Li-Cor Bioscience)
Phosphate Buffered Saline (PBS)	130mM NaCl, 28mM KCl, 10mM Na_2HPO_4, 1.8mM KH_2PO_4, pH 7.4

iBIND™ Solution	1% iBind 100X Additive, 20% iBIND 5X buffer

2.11.5 Solutions for luciferase ATP assay

Table 14: Solutions used for detecting ATP release.

Solution	Composition	Source
Standard Reaction Solution	• 8.9 mL dH2 O • 0.5 mL 20X Reaction Buffer (Component E) • 0.1 mL 0.1 M DTT (from step 1.3) • 0.5 mL of 10 mM D-luciferin (from step 1.2, store the remaining 0.5 mL at ≤–20°C for up to several weeks) • 2.5 µL of firefly luciferase 5 mg/mL stock solution	Life Technologies

2.11.6 Solutions for OE and VNO stimulation

Table 15: Solutions used for OE and VNO Stimulation.

Solution	**Concentration**	**Source**
Ringers	See appendix B	
Henkle 100	1:10000	Germany
Potassium gluconate	25mM	Sigma
ARL 67156 trisodium salt hydrate	100uM	Sigma

2.11.7 Solutions and media for dye uptake

Artificial cerebral spinal fluid (ACSF) – 119 mM NaCl; 26.2 mM $NaHCO_3$; 2.5 mM KCl; 1 mM NaH_2PO_4; 1.3 mM $MgCl_2$; 10 mM glucose; 2.5-mM $CaCl_2$.

2.12 Consumables

Table 16: Cell culture Consumables.

Product	**Company of Retrieval**
Petri Dish (Coated) for Cell Culture	Falcon®
6 cm TC-Treated Dish for Cell Culture	Falcon®
24 Well TC-Treated Cell Polystrene Permeable Support Companion Plate With Lid (Sterile)	Falcon®
Cover Slips	Fisher Scientific
Glass Slides	Fisher Scientific

96 Well TC-Treated Cell Polystrene Permeable Support, Black Clear , Flat Bottom With Lid (Sterile)	Greiner BioOne
96 Well TC-Treated Cell Polystrene Permeable Support, White , Flat Bottom With Lid (Sterile)	Greiner BioOne
Multipipette troughs	VWR
Filter pipettes (5, 10, 25mL)	Corning, Falcon
Serological pipettes (5, 10, 25 ml)	Fisher Scientific
Plastic consumables (pipette tips, Eppendorf tubes)	Fisher Scientific, Qiagen

Table 17: General consumables.

Product	**Company of Retrieval**
Bent Glass Rods	Sigma-Aldrich
Glass Pipettes	Eppendorf
Plastic Agar Plates	Fisher Scientific
Plastic Consumables	Sarstedt and Fisher Scientific
Plastic Cuvettes	VWR
Whatman filter paper	Macherey-Nagel
Syringe filters (22µM)	Omnilab

2.13 Equipment

2.13.1 Equipment for dissection

CO_2 chamber

Metal tools (scissors, scalpel, and tweezers)

Incubator Heratherm (Thermoscientific)

2.13.2 Equipment for cell culture

Table 18: Equipment for cell culture.

Equipment	**Title**	**Company**
Water Bath		VWR
Laminar flow unit	1300 Series A2	Thermo Scientific
Light Microscope	CKX41	Olympus
Confocal Microscope	LSM 700	Zeiss
Incubator	Formula Steri-Cycle CO_2 Incubator	Thermo Scientific

Hemocytomer		La fontaine
Lab centrifuge and rotor	Cetrifuge 3-15 and rotor 11133	Sigma

2.13.3 Equipment for molecular biology

Table 19: Equipment for molecular biology.

Equipment	Title	Company
Bacterial Shaker	Innova40	New Brunswick
CO_2 cell culture Incubator	HERA THERM	Thermo Scientific
37°C Bacterial Incubator	Single-cell electroporator	Eppendorf
Lab Centrifuge	Sorvall Legend Micro 21R	Thermo Scientific
PCR Machine	Mastercycler Nexus X1	Eppendorf
UV Gel Documentation System	Alpha Imager HP System	Fisher Scientific
Water Bath	Isotemp 210	Fisher Scientific
Weghing Scale	Navigator	OHAUS
Magnetic Stirrer and Hot plate	Isotemp	Fisher Scientific
Electrophoresis Tank and Current Supply		BIO RAD
Photospectrometer	Nanodrop 2000	Thermo Scientific
Cell imaging camera	Infinity1 UTVIX-2	Olympus
Rocking platform	Model 100	VWR
Vortex mixer		Fisher
Nucleic acid purification system	Qiacube	Qiagen
Nanodrop 2000 Photosceptrometer		Thermo Scientific
Agarose gel electrophoresis	Mini-sub cell GT	Biorad

2.13.4 Equipment for protein biochemistry

Table 20: Equipment for protein biochemistry.

Equipment	Title	Company
Blotting Chamber	Trans-Blot Turbo Transfer System	BioRad
Infrared Western Blot Scanning System	Infrared: Odyssey Infrared Imaging System	Li-Cor Biosciences
Blotting Membrane	Nitrocellulose Starter Kit	BioRad
Protein Purification System	QIAcube System	Qiagen
Nitrocellulose membrane	Transblot Turbo Transfer Pack	Biorad

2.13.5 Equipment for microscope analyses

Table 21: Equipment for microscope analyses.

Equipment	Title	Company
Light microscope	Olympus BH-2	Olympus
Camera	Olympus DP71	Olympus
Confocal Laser Scanning Microscope	LSM 510 META	Zeiss
Mounting Slides	Superfrost Plus Slides	Fisher Scientific

2.13.6 Equipment for fluorescent and luminescent assays

Table 22: Equipment for fluorescent and luminescent assays.

Equipment	Title	Company
Multi-Mode Microplate Reader	Synergy H4	BioTek
pH detection	pH Pro	Mettler Toledo

2.14 Software

Image processing	ImageJ, Adobe Photoshop and Illustrator CS6
Primer Design and PCR Analysis	NCBI/Primer-BLAST
Analyses of DNA sequences	Eurofins Genomics, DNA
Protein sequence alignments	Clustal
Image acquisition and processing	ZEN 2010 (Carl Zeiss Microscopy)
Image acquisition with the Olympus	cell^{A} software © Olympus
Luminescence Assay	Gen5
Fluorescence Assay	Gen5
Assay Statistical Analysis	Microsoft Excel 2013
DNA Concentration	Nanodrop2000
Gel documentation	AlphaImager
Primer design	NEBaseChanger
Text processing	Word 2013

3. Methods

"My methods are really methods of working and thinking; this is why they have crept in everywhere anonymously."

- Emmy Noether

3.1 Molecular biological methods

3.1.1 Cloning of DNA fragments

3.1.1.1 Bacterial cultivation

Recombinant bacteria was collected and seeded (50-100 µl depending on the strength of expression of the PCR product) onto LB-agar plates containing kanamycin antibiotic (50 µg/ml, Table 11) (BioShop); then incubated ON at 37°C to obtain single clones. For preparative production of recombinant plasmid DNA, single colonies were picked with pipette tips and transferred into 5 ml of LB growth media (Table 11) and were incubated in an angled horizontal shaker ON at 37°C at 250rpm.

3.1.1.2 Determination of nucleic acid and protein concentration

To determine the concentration of DNA, the absorbance at 260 nm (A260) was measured with a Nanodrop 2000 photospectrometer using 1µL of preparation. Purity of the DNA was also determined by measuring the absorbance at 280nm. The quotient A260/A280 specifies contaminations; values close to 1.8 indicate pure DNA.

3.1.1.3 Plasmid DNA preparation

For completing DNA sequencing of both transient and stable transfection, there is a demand for highly purified DNA. For analytical and preparative purposes, DNA was prepared small-scale from *E. coli* bacteria. Once the bacterial ON culture was complete, it was pelleted to compact the bacteria and collect it. In order to do this, 2 ml was collected, centrifuged at 14 000 rpm for 3 minutes at RT, and the supernatant was removed. This was repeated once more, in order to collect a sufficient amount of bacteria. Pellets were then suspended following the QIAPrep Spin Miniprep Kit manufacturer's guidelines. The QiaCube, along with the Miniprep kit, was used to

facilitate the extraction of highly purified, endotoxin free plasmid DNA. Typically ~200ng/µL, plasmid DNA was obtained from 4ml ON cultures. DNA remained at -20°C until use.

3.1.1.4 Amplification of DNA fragments by PCR

Amplification of specific DNA fragments were completed by polymerase chain reaction (PCR) during site directed mutagenesis. In order to conduct this, the Q5 Hot Start High-Fidelity DNA Polymerase from the kit was used to ensure that the reaction is completed efficiently and with a low error rate. Forward and reverse primers were diluted to a final concentration of 10 µM in DNase/RNase free water. See table 23 for PCR solution composition, table 24 for cycling conditions, and refer to section 3.2 for full experimental details.

Table 23: Exponential Amplification of DNA fragments by PCR.

Solution	Total volume 25 µl	Final Concentration
Q5 Hot start High-Fidelity 2x Master Mix	12.5 µl	1X
10µM Forward Primer	1.25 µl	0.5 µM
10 µM Reverse Primer	1.25 µl	0.5 µM
Template DNA 10ng/ µl	1 µl	10ng
Nuclease-Free water	9.0 µl	

Table 24: PCR cycling conditions.

Step	Temperature	Time
Initial denaturation	98°C	30 seconds
30 cycles – denaturation Hybridization Elongation	98°C 72°C 72°C	10 seconds 30 seconds 30 seconds/kb
Final Extension	72°C	2 minutes
Hold	4°C	

3.1.1.5 Agarose gel electrophoresis

To confirm presence of PCR products, DNA samples in 1x FastDigest green buffer were electrophoresed on 1.0% agarose gels containing 0.1 g/ml ethidium bromide, in submarine gel electrophoresis chambers. To confirm size standards, samples were run against a 1kB ladder. 1X TAE was used for the running buffer, and gels were run at 100 V for approximately 1 hour. Images of the gel were captured using the Alpha Imager HP system.

3.1.1.6 Kinase, Ligation and DpnI of DNA fragments

Ligation was preformed according to the protocol in the Q5 Site-Directed Mutagenesis Kit with no changes, after addition of the kinase and before the addition of DpnI. These enzymes were mixed together as part of a unique enzyme mix (KLD) from NEB. See section 3.2 for full details.

3.1.1.7 Transformation of plasmid DNA into competent bacteria by heat shock

To efficiently produce recombinant plasmid DNA, competent DH5α-T1 *E. coli* bacteria was used, which was manufactured in advance to be chemically competent via NEB. Once the bacteria was thawed on ice, 5 µl of KLD mix was added to the cells and carefully flicked 4-5 times to ensure the two components were appropriately mixed. This combination of cells and KLD mix was then kept on ice for 30 minutes, followed by heat shock at 42°C for 30 seconds. This heat shocked mixture was then kept on ice for 5 minutes and once complete, was ready to be incubated in 950 µl of RT SOC media at 37°C for 60 minutes with shaking (250rpm).

3.1.1.8 Plasmid DNA preparation

To isolate plasmid DNA from 5ml DH5α overnight culture, the QIAPrep Spin Miniprep Kit was used based on guidelines from the manufacturer.

3.2 Site directed mutagenesis

Site directed mutagenesis was used in order to create the numerous Panx1a mutations to allow functional analysis of the Panx1 protein. Primers were designed accordingly – ie. with an alanine (A) or histidine (H) point mutation using NEBaseChanger™ to confirm primer design and calculate annealing temperatures (Table 8). An important note for primer designs that contain substitutions include; incorporating the nucleotide changes in the center of the forward primer with at least 10 complementary nucleotides on the 3' side of the mutation and designing the reverse primer so that the 5' ends of the two primers anneal back-to-back. Once primers were designed and ordered, the Q5® Site-Directed Mutagenesis Kit was used (New England BioLabs), enabling rapid, site-specific mutagenesis of double-stranded plasmid DNA. The kit contains a Q5® Hot Start High-Fidelity DNA Polymerase, which in combination with the mutagenic primers, creates insertions, deletions and substitutions in the desired template plasmid – i.e. pEYFP-

drPanx1a, during polymerase chain reaction (PCR). PCR was conducted for amplification of the DNA coding region fragments according to the protocol contained in the kit. A few minor changes to the standard protocol include; using 10µM final concentration of the primers and 10ng of template DNA in the PCR reagent mix, using 30 cycles in the PCR thermocycling conditions, annealing temperatures were used according to NEB and only altered according to improper PCR results (ranging between 61-70°C), with 3 minutes of cycling at 72°C during annealing (calculated based on plasmid length) (Table 8). A 1% agarose gel was run to confirm presence of the PCR product before continuing with mutagenesis. For circularization of the PCR product and removal of the template DNA, a unique enzyme mix containing a kinase, ligase and DpnI was added to the PCR product and incubated according to protocol; creating a KLD mix. In order to efficiently transform plasmid DNA into competent bacteria (NEB 5-alpha *E.Coli*), the enzyme mix was used and standard heat shock protocol was followed. Once colonies were grown in SOC media and inoculated (50-100µL depending on how much PCR product was visible on the gel) on agar plates containing kanamycin antibiotic (1:1000), single colonies were picked for analytical and preparative production of recombinant DNA according to Q5 Qiagen mini-prep protocols using the QIAcube (Qiagen). Glycerol stocks were made from the bacteria containing correct plasmid expression that were confirmed with professional sequencing by Eurofins Genomics. Mutations that were created using this method are shown in various applications in section 4.2.

3.3 Sequencing of plasmid DNA

Sequencing of plasmid DNA was done commercially by Operon-Eurofins MWG. After sequencing, raw sequences were aligned to Panx1a using ClustalW.

3.4 Bioinformatics

DNA sequences were identified using the nucleotide search function of the National Center for Biotechnology Information (NCBI; http.//www.ncbi.nlm.nih.gov). Once sequences were obtained, they were subjected to the multiple sequence alignment tool, ClustalW2, where subsequent analysis inspired primer designs. Primers were drafted using NEBaseChanger™. Predictions of structural analysis and interacting binding regions were gathered using ELM

resources. Protter was used to produce a visual representation of the amino acid sequence of Panx1a, highlighting important mutated regions (See section 4.2 for examples). 3D structure predictions were attained from Bloomsbury Centre for Bioinformatics (Appendix G).

3.5 Cell culture

3.5.1 Culturing N2a cells

The mouse neuroblastoma cell line, Neuro2A (N2a), was cultivated in supplemented DMEM (Table 9) at 37°C and 5% CO_2 in a humidified atmosphere. Cells were passaged routinely every three to four days according to the following protocol in 10cm tissue culture treated petri dishes. First, DMEM was removed from the culture and N2a cells were washed carefully with PBS (without calcium and magnesium). Subsequently, cells were incubated with 400µl trypsin for at least 2 minutes with agitation applied to the culture dish for the duration of the incubation. Once cells visually appear to be detached from the dish, 5ml of fresh, warmed media is added and cells are split using mechanical stimulation via the pipette. Finally, 1ml of the cell suspension is collected and seeded into a new 10cm dish containing 9ml of fresh media. This passaging process is repeated until approximately P30, which is when new cells are thawed and cultured. For experimentation purposes, cells are seeded into variously sized well plates (24 well, 96 well and 6cm) at standard cell densities.

3.5.2 Transient transfection

Transient transfection was performed using the Effectene Transfection Reagent Kit (Qiagen) according to manufacturer's guidelines. Cells were seeded 1 day prior to transfection, for dye uptake assays they were seeded at 15 000 cells in 96 well plates, for whole cell lysates used for western blots 30 000 cells were seeded in 24 well plates, and for confocal microscopy 20 000 cells were seeded in 24 well plates. Transfection was carried out the next day, using 100-200 ng of highly purified plasmid DNA, and cells were taken for experiments 48 hours post transfection. It is important to note that protocol typically states that one should wash cells in PBS prior to replacing media and continuing with transfection, however, due to the nature of these experiments this was not completed.

3.5.3 Stable transfection

Stable transfection cell lines are achieved by initiating a desired transient transfection, as stated in section 3.5.2, in cell culture. Cells are then cultured according to section 3.5.1, however, supplemented DMEM also contains 300mg G418 to kill off any cells not expressing the drug resistance gene neomycin-S-transferase (Neo).

3.6 Protein biochemical methods

3.6.1 Preparation of lysates and Western blot completion

To confirm protein expression using western blotting techniques, mouse neuroblastoma cells (N2a) were cultivated in Dulbecco's Modified Eagle's Medium (DMEM) with high glucose and additionally supplemented with L-glutamine, 10% fetal bovine serum (FBS) and non-essential amino acids (NEA). Once cells were passaged according to standard protocol, plated in 24-well plates, and were visibly confluent, they were transiently transfected with either ~200ng Panx1a, EYFP, or the various mutants (Table 8) according to the life technologies protocol using the reagents found in the kit (effectene, enhancer and EC buffer). After 48 hours post transfection, DMEM was removed from the cells, and they were lysed with 100µL 1x laemmli. Lysates were incubated and denatured at 95°C for 5 minutes and placed on ice for 1 minute prior to loading. 4µL of a protein marker and 15µL of lysates were loaded for each experiment after the 10% separation and comb gels were created for gel electrophoresis of the proteins; following standard protocol. Gels were run in the SDS-PAGE chamber at 100 V for approximately 1-1.5 hours, transferred onto a nitrocellulose membrane using the BioRad Trans-Turbo™ Transfer System and underwent immunoblotting in the iBind™ Western System according to the protocol provided by life technologies. Reagents used during the western blot procedure included primary antibodies GFP and β-actin at dilutions 1:200 and 1:3000 respectively, and secondary antibodies rb680 and m800 at 1:3000 and 1:2000 respectively. Once the membranes were finished being washed and probed with the blocking solution and antibodies, the blot was imaged using the Odyssey ® CLx Infrared Imaging System, which uses licor software, to fluorescently image the blot. Examples of images produced from this procedure are shown in figures 15 & 23.

3.7 *In vitro* high throughput fluroescent dye uptake assay in N2a cells

The purpose of using the synergy for analyzing high throughput dye uptake behaviour in Panx1a, EYFP and mutants under varying environmental conditions, was to mirror conditions as similarly as possible to the confocal single cell imaging technique. This was to allow one to gather both quantitative and qualitative data in an efficient manner. That being said, a few variances did exist. For instance, N2a cells were cultured in DMEM lacking phenol red and mutants were transfected in the same manner as previously mentioned. However, Panx1a and Eyfp cultures were cultivated from a stable transfected cell line containing G418 in the media. Moreover, instead of seeding in 24-well sized Matek plates, all cells were plated in 96-well plates with clear, flat bottoms and black sides, with approximately 60 000 cells seeded per well and a 48 hour growing period. All solutions were made in artificial cerebral spinal fluid opposed to DMEM, with the same EtBr concentration (10μM). pH values were kept consistent, using pH levels 4.5, 6, 7.4, 8.5 & 10.2.

In order to conduct fluorescent dye uptake with the synergy H4 microplate reader it must be initially set to an internal temperature of 37°C, and the plate (wells A1-H12) is 'read.' When a read step is defined it means setting the machine to conduct fluorescence, an endpoint reading of each well, normal scan time per well, excitation at 540 +/-20, and emission at 620 +/-20, optics set at the bottom and a gain of 100. Once an initial read of the plate is completed (a reading of cells in the cultured DMEM acts as our background value), the plate is set to eject to allow the removal of the supernatant from the cells, followed by the application of the various pH adjusted ACSF solutions containing EtBr to the appropriate wells. Subsequent reads are defined according to the same parameters mentioned prior, with 20 second delays in between each read. This alternating read and delay process is repeated until 50 cycles have been completed. The output reading is exported to excel and is displayed in fluorescent units, depicting the amount of dye that is taken up into the cell. Data has been represented as a time course with values normalized to the original background reading and scaled to time = 0.

3.7.1 Analysis of dye uptake assays

Recordings gathered from Gen5 using the synergy H4 were exported to Excel for analysis. First, a background reading is conducted with the cells, prior to the addition of solutions with EtBr, to act as a normalizing value. When the cells that are not fluorescing are compared to subsequent readings of those cells that are, it aids in the removal of them from the data analysis in order to prevent skewing of the data, hence doing the background read first. Once the first read is completed, according to protocol mentioned in 3.7, this is used as the second normalizing value in order to take this as time point 0 in our time course. Each plate has 8 well replicates of cultured cells, with a confluence of approximately 60 000 cells per well, per experiment. Replicates are averaged across each individual time point. Standard statistical analysis allows the elimination of outliers, and determines significance. The student's t-test was used to test for statistical significance, confidence limit being 0.05. Figures were prepared using typical box plot procedures for Excel, as this is important for providing a visual representation of how the data for each population is distributed, giving interquartile ranges to indicate error.

3.8 Zeiss confocal microscopy

Fluorescent confocal microscopy was performed using a ZEISS LSM700 microscope. ZEISS ZEN software was used to control all parameters during imaging. Identical imaging parameters (i.e. Gain settings, exposure, magnification, etcetera) were used to allow direct comparisons of OE and VNO IHCs from Panx1 +/+ and Panx1 -/- mice; as well as fixed Panx1a expressing cells to alanine and histidine mutants in N2a cells. Lasers 488nm and 405nm were used in order to image green fluorescent protein (GFP), which is C-terminally tagged to our protein of interest, and DAPI to show our nuclei, in green and blue respectively. LSM images were exported into tiff format and assembled using Photoshop CS.

3.8.1 Fluorescent dye uptake: confocal microscopy for single live cell imaging

In order to analyze the dye uptake behaviours of Panx1a, EYFP and mutants under varying environmental conditions, N2a cells were cultured and transfected in the same manner as mentioned before. However, cultures were equilibrated for 15 minutes in 1 mL DMEM lacking phenol red prior to use, to avoid cross-talk between the phenol red and ethidium bromide dye

(EtBr) during fluorescent imaging. It is important to note that this method was employed to test the effect of varying external pH levels on cells with Panx1a in culture. The experimental procedure required 10µM of EtBr to perform the dye uptake, and DMEM with supplemented FBS was used for varying the environmental pH levels in pH sensing trials. Experimental pH levels used included pH 5, 6, 7 & 8. During confocal imaging at magnification 40x, reflectors for DAPI, GFP and Texas Red were activated to view nuclei (blue), protein (green) and EtBr dye (red), and a field of view containing approximately 6-10 transfected cells were focused on. To initiate the dye uptake process, 1 mL of DMEM solution, including the EtBr and desired pH, was added carefully to the cell culture dish and images were recorded every 20 seconds for 50 cycles. It is important to note that control conditions, Panx1a with pH of 7.4, were completed first in order to optimize the imaging controls in the ZEN 2010 program. Subsequent trials were completed with Panx1a and varying extracellular conditions – i.e. increasing or decreasing pH. Post imaging, MEAN ROI were selected in the membrane, as well as the intracellular and extracellular environments of the cells to allow for determining the amount of EtBr uptake into the cell. To complete dye uptake experiments, pictures of the cells were taken and analyzed in ImageJ. For statistical analysis N ≥ 20cells were analyzed for each condition using ZEN 2010 software, ImageJ and Excel.

3.8.2 Localization studies of Panx1 and mutants in N2a cells

To determine protein localization using fluorescent microscopy, mouse neuroblastoma cells (N2a) were cultivated in (DMEM) and were transiently transfected with either ˜200ng Panx1a, EYFP, or the various mutants (Table 8); it is important to note that all constructs contained a fluorescent tag allowing for microscopy. After 48 hours post transfection, DMEM was removed from the cells; they were washed with 500uL PBS +/+ 2 times, and incubated in 10% formalin for 30 minutes. Once fixation was complete, coverslips were removed from the wells and mounted with 6µL of DAPI staining mounting media on slides. Slides were left to set over night at 4°C in the dark and then imaged using the ZEISS LSM 700 confocal microscope, coupled with the ZEN 2010 computer software, which uses lasers for reflecting DAPI and GFP to capture fluorescently stained nuclei (in blue) and protein (in green) respectively. All images were taken at 63x magnification using immersion oil. It is important to note that wild type samples were

imaged first, in order to scale all other samples against the exposure and gain settings gathered from controls. Examples of collected images, that were later processed using ImageJ and Photoshop CS6 for presentation, can be seen in figures 16 and 24.

3.8.3 Localization studies of Panx1 in olfactory epithelium and vomeronasal organ

To determine protein localization using fluorescent microscopy, in WT and Panx1 KO mice populations in the OE and VNO, proceedings were similar to those outlined above. 12µm cryosections were collected from each population in the two different regions of interest, and they underwent IHC, as outlined in 3.13. Microscopy was completed to standard protocol ensuring the highest quality picture settings were entered for image capturing, processing was completed with ImageJ and Photoshop CS6.

3.9 Dissection of Panx +/+ and -/- mice populations

After the mice were sacrificed according to Canadian Council on Animal Care guidelines, the skulls of the mice were detached and the roof of the mouths were removed in order to isolate the VNO. Full dissection of the VNOs were conducted in Ringers solution under a dissecting microscope to ensure no mechanical stimulation or damage occurred to the structure while removal of the entire boney capsule was completed. Once isolated, they were stored in Eppendorf tubes containing fresh Ringers. For OE isolation, after mouse skulls were retrieved, they were dissected parasagittal to the septum to carefully expose the nasal cavity and the intact OE. Note, some septal and olfactory mucosa removal was required after dissection down the midline, depending upon the nature of the dissection, to fully expose the turbinates.

3.10 qPCR

RNA was isolated from adult male mice using the RNAeasy Fibrous Tissue Mini Kit (Invitrogen, Canada) and cDNA was synthesized from 1µg of RNA with the ReadyScript cDNA Synthesis Kit (Sigma-Aldrich, Canada), according to the manufacturer's instructions. qPCR was performed using the SsoFast EvaGreen Supremix (Bio-Rad, Canada) and the following oligonucleotide pairs: Panx1fw: CAGGCTGCCTTTGTGGATTC Panx1rev: CGGGCAGGTACAGGAGTATG Panx2fw: GGTACCAAGAAGGCCAAGACT Panx2rev: GGGGTACGGGATTTCCTTCTC Panx3fw:

CTTACAACCGTTCCATCCGC Panx3rev: CAGGTACCGCTCTAGCAAGG 18Sfw: TGACTCTTTCGAGGCCCTGTA 18Srev: TGGAATTACCGCGGCTGCTG. fw = forward, rev = reverse, 18S served as the reference gene. Experiments were performed in triplicates, using three OE and brain samples. Relative gene expression was calculated using the REST software (2009) (Pfaffl, Horgan, & Dempfle, 2002).

3.11 Solution application and collection of ATP samples

3.11.1 Extracellular ATP from OE of Panx +/+ & -/- mice

For sample collection, once successful removal of the septum was completed, the OE was entirely exposed while it remained undamaged; the tissue was then placed in a horizontal upright orientation to allow proper experimentation and application of the various solutions. The OE was placed upside down for extracellular ATP extraction. Since the OE rapidly degenerates once axons get transected, this *ex vivo* preparation was required instead of a more invasive dissection procedure, in order to extract extracellular ATP from the cilia surface. To avoid mechanical stimulation, which would elicit ATP release in itself, small droplets (25µl) of Ringers solution (see appendix B for recipe), H100 (Henkel 100, 1:10000 in Ringers solution, Henkel, Germany (Wetzel et al., 1999)), and potassium gluconate (Pglu) (25mM, Sigma-Aldrich, diluted in Ringers solution) were subsequently and gently pipetted onto the cilia surface at the center of the OE. Each solution contained 100µM ARL 67156 trisodium salt hydrate (Sigma-Adlrich) to inhibit ATPases and allow for sufficient measureable levels of ATP. The tissue was equilibrated in Ringers for 3 minutes and subsequently incubated in H100 and Pglu for 90 seconds per trial; 10µl samples from each application were carefully collected. Samples were heated at 95°C for 1 min after extraction, flash frozen on dry ice and stored at −80°C until use. Between solution applications, droplets of previous solutions were fully removed. It is important to document that this methodology was a novel development, as no one to date had previously reported being able to reliably measure extracellular ATP levels *ex vivo.* Sample sizes for this experiment were as follows; N=7 for WT in Ringers, no inhibitor. N=8 and 7 for WT and KO, respectively, in Ringers and inhibitor. N=10 for both WT and KO with H100 stimulation. N=10 and 9 for WT and KO, respectively, for Pglu stimulation.

3.11.2 Extracellular ATP from VNO of Panx +/+ & -/- mice

Once VNOs were successfully isolated and stored in Ringers solution, enough to be fully submerged (1000µl), they remained there for 3 minutes for equilibration. The Ringers solution was replaced with fresh Ringers in both the stimulated and non-stimulated conditions for both mouse populations. For those that were non-stimulated, they remained at rest in the Eppendorf tubes undisturbed for 10 minutes. For the samples that were mechanically stimulated, the surrounding Ringers solution was carefully pipetted up and down around the VNO for a consecutive 10 minutes, ensuring not to capture or disrupt the VNO. After the incubation time was complete, 50µl of the supernatant was removed, heated for 1 minute at 95°C, and stored on ice until it was used in a luciferase assay. Six VNO biological replicates were used for each population.

3.12 *Ex Vivo* high throughput ATP luciferase assay

To measure ATP levels in the samples, a high-throughput luciferase based assay technique was used. ATP assays were performed in a 96 well format using the Molecular Probes® ATP Determination Kit (Life Technologies, USA) and the Synergy H4 hybrid multiwall plate reader (Biotek, USA). Samples were slowly defrosted on ice and pipetted quickly into a white flat bottom 96 well plate (Greiner Bio-One, Canada) that was also kept on ice. Luciferase Reaction Buffer was made according to standard protocol (see appendix B for details) and 100µl was added to each well containing 10µl of sample. The plate was then placed in the Synergy and was set to read each well according to standard luminescence protocol set by the Gen5 Data Analysis Software (BioTek), with automatic gain settings and 5 seconds integration time per well. Data was exported from Gen5 to excel for analysis and ATP concentrations were determined from the ATP standard curves included in each assay (concentrations: 0µM, 1 µM, 5 µM, 10 µM & 25 µM of ATP dissolved in TE buffer was used for standardization); the student's t-test was used to test for statistical significance.

3.13 Immunohistochemistry (IHC)

Once adult male mice were sedated with carbon dioxide and euthanized via cervical dislocation, their heads were decapitated and their fur and palate were removed. The heads were then fixed in 4 % PFA at 4°C overnight (ON) and dehydrated in 30 % Sucrose at 4°C ON. 12 µm cryosections were prepared, and for antigen retrieval the fixed cryostat sections were incubated for 5 minutes with 1% SDS, followed by three washes each for 5 minutes with PBS. Sections were blocked with 5 % normal goat serum (NGS), 1% bovine serum albumin (BSA), and 0.1% Triton X100 in PBS for 1 hour at room temperature (RT). The primary antibody (1:100, Dr. Penuela from the University of Western Ontario) was applied in 1 % BSA in PBS containing 0.1 % Triton X-100, at 4°C ON. After the ON incubation, specimen were carefully washed three times with PBS for 10 minutes each, and the secondary goat anti-rabbit Alexa Fluor 488 (Invitrogen, Germany) antibody, diluted in PBS (1:1000), was applied for 30 min at RT in the dark. After three 10 min washes with PBS, with the container was kept away from light, sections were briefly dried and embedded in ProlongGold Antifade (Invitrogen, Germany), mounted and cover slipped with DAPI (Sigma Aldrich), kept at 4°C ON in the dark and imaged using confocal microscopy. The Laird laboratory generously provided the primary antibody for Panx1 IHC (Penuela et al., 2007).

4. Results

``It has been said that you can`t understand biology until you understand evolution. I would argue that you can`t understand evolution or biology until you understand protein. ``

- Susan Lindquist

4.1 Understanding ATP release from Pannexin1 in an animal model

4.1.1 Pannexin expression in the brain and olfactory epithelium

Purinergic signaling is very important for the perception of sensory stimuli, making ATP a main player in modulating sensory systems through multiple mechanisms; including modulating sensory sensitivity, signal transduction, neurotransmission and even gap junctional coupling (Bobbin and Thompson, 1978; Munoz et al., 1995; Zhu and Zhao, 2012). The mechanism of ATP release is still poorly understood, however, the role of ATP release via Panx1 has been alluded to in a few sensory systems. Therefore, we aimed to investigate this role in the olfactory system. Thus far, it is understood that in the OE extracellular ATP causes intracellular calcium levels to rise in the olfactory sensory neurons (OSNs) to suppress odour responsiveness (Hegg et al., 2013). A similar event occurs in the VNO, however, ATP activates P2X receptors in order to initiate this cascade of events (Vick and Delay, 2012). To start our investigation we had to confirm the expression of Panx1 in the brain and OE of mice. Using primers specific for Panx1 and Panx2, we used qPCR to investigate this (Figure 8). Significant expression of Panx1 mRNA was detected in the OE and whole brain lysates of wild type mice. Meanwhile, no expression of Panx1 was detected in the brain or OE of Panx1 -/- animals – confirming the loss of Panx1 (Figure 8A). Primers were used to detect Panx2, to address the possibility of compensatory mechanisms that may occur with a KO population. According to figure 8B, there is no significant difference seen in the expression of Panx2 in the brain of either population. Meanwhile, no expression is found at all in the OE of Panx +/+ and -/- mice, meaning Panx2 expression is significantly different to Panx1 found in this region and to the amount of Panx2 seen in the brain ($p<0.001$). There were no detected levels of expression of Panx3 in either of these regions; as a result this was excluded from the figure. Since qPCR was able to confirm Panx1

expression in the olfactory system, and there is no indication of upregulated family members, it gave us a foundation to pursue the determination of specific localization of the protein.

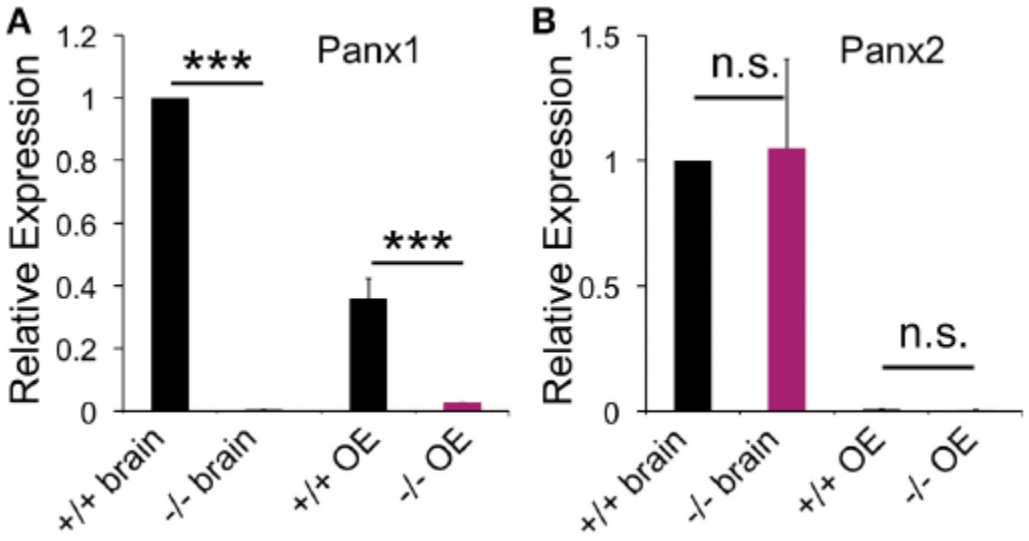

Figure 8: Pannexin expression in the brain and olfactory epithelium. qPCR data for pannexin expression in the OE (N=3) and brain (N=3) of adult male mice. **A)** Panx1 -/- mice lacked Panx1 expression in both the brain and OE. **B)** No difference was detected in Panx2 expression of both populations in the brain, meanwhile, no Panx2 expression was found at all in either Panx1 +/+ or Panx1 -/- populations in the OE. Panx3 expression was not detected or shown. Primers specific for 18S were used as the reference. Experiments were performed in triplicates. ***p < 0.001. n.s., not significant. Error bars: s.e.m.

4.1.2 Localization of Pannexin1 in the olfactory epithelium

With the expression of Panx1 confirmed in the OE of Panx1 +/+ mice, it fuelled us to pursue localization studies. Previously, *in-situ* hybridization technology and cRNA specific mouse Panx1 probes were used by Ray et al (2006) to show that there is strong staining present in the olfactory sensory layer (OSN) of the OE. Therefore, we aimed to validate this mRNA localization data using immunohistochemistry (IHC) and a specific antibody for Panx1 (graciously provided by S. Peneula, Western University). For the first time in Panx +/+ animals, IHC of the OE revealed prominent Panx1 staining (green) in the axon bundles of the OSNs, which project to the olfactory bulb (Figure 9). Virtually no staining was found in the same region of Panx -/- mice, significant differences are indicated by asterisks (Figure 9). There is a diffuse background

signal present in the basal, neuronal and sustentacular cell layers, however, there is much more prominence in the wild type population. Surprisingly there was no pronounced staining found in the OSN cilia, which are native regions to OSN signaling and depolarization after odorant activation – where ATP is proposed to play a paracrine signaling role. However, since Panx1 was visualized in the axon bundles that project to the olfactory bulb, it had us questioning if the VNO was playing an interactive role in this system and the proposed Panx1 mediated olfaction process.

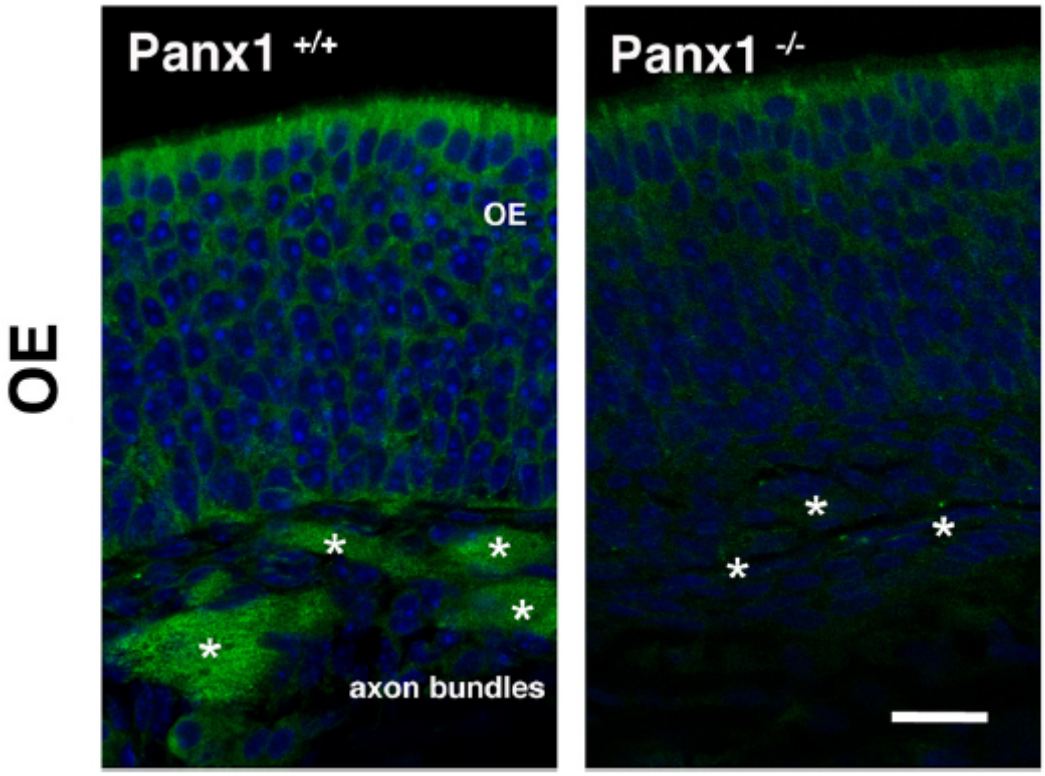

Figure 9: Localization of Panx1 in the olfactory epithelium of Panx1 +/+ (left) and Panx -/- (right) mice using immunohistochemistry. Collecting cryosections from the OE of the fixated heads of Panx1 +/+ and Panx1 -/- mice in order to conduct immunohistochemistry techniques using a primary antibody generated by Dr. Penuela to confirm specific localization of Panx1. **Left)** In the OE, prominent Panx1 staining (depicted in green) was identified in the axon bundles of the OE (asterisks), which was not detected in the Panx-/- mice **(Right)**. Nuclei were stained with DAPI (in blue). Images were recorded with Zeiss LSM700, using identical conditions. Images were extracted and processed using imageJ. Scale bars = 200 µm Nuclei were stained with DAPI (in blue). Images were recorded using identical conditions. Scale bars = 200 µm

4.1.3 Localization of Pannexin1 in the vomeronasal organ

Using the same IHC technique, we observed a strong staining of the sensory cell layer in the VNO of Panx1 +/+ compared to Panx1 -/- mice, indicated by asterisks (Figure 10). It is important to highlight that determining specific localization of Panx1 in the two olfactory systems was extremely novel. Moreover, based upon the expression patterns of Panx1, it was rational to assume that the protein was capable of playing a role in olfaction, making it logical to continue with functional analysis experimentation.

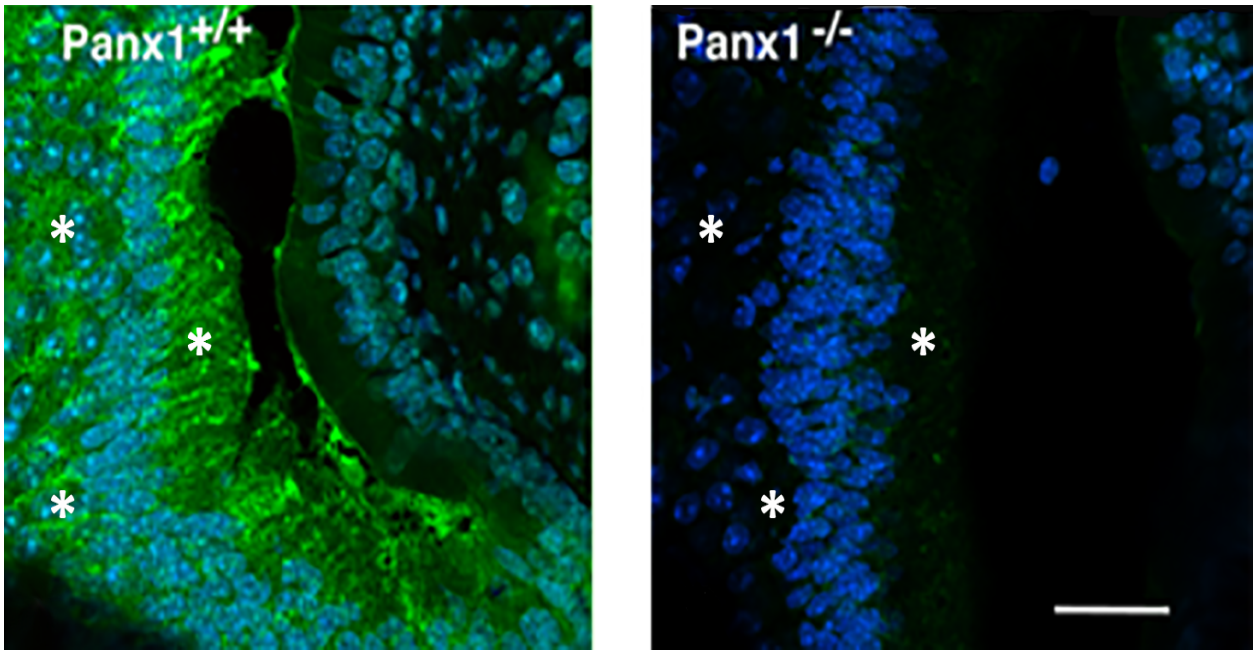

Figure 10: Localization of Panx1 in the vomeronasal organ of Panx1 +/+ (left) and Panx -/- (right) mice using immunohistochemistry. Collecting cryosections from the VNO of the fixated heads of Panx1 +/+ and Panx1 -/- mice in order to conduct immunohistochemistry techniques using a primary antibody generated by Dr. Penuela to confirm specific localization of Panx1. **Left)** In the VNO, prominent Panx1 staining (depicted in green) was identified in the sensory cell layer (asterisks), which was not detected in the Panx-/- mice **(Right)**. Nuclei were stained with DAPI (in blue). Images were recorded with Zeiss LSM700, using identical conditions. They were extracted and processed using imageJ. Scale bars = 200 µm

4.1.4 Quantification of extracellular ATP release from olfactory epithelium

Coupling the fact that localization of Panx1 was confirmed, with the well-known fact that Panx1 is a major ATP release channel, it was only practical to use a luciferase based ATP assay to discriminate the function of the Panx1 channel in the OE *ex vivo.* It is important to note that during this procedure an ATPase inhibitor was applied to the stimulating solutions; to aid in the prevention of ATP break down in order to gain reliable readings of ATP efflux in the pM range. Application of the inhibitor increased ATP levels more than 100 fold when compared to the physiological condition with no inhibitor present (Figure 11). Serial application of Ringers solution, Henkel100 (H100) and potassium gluconate (Pglu) to both Panx +/+ and -/- mice revealed interesting results. No significant differences (p=0.66) were found in ATP detection

between populations upon the application of physiological Ringers solution, as expected. In addition, when H100 was used to stimulate the OE, again, no significant differences ($p=0.78$) in ATP release were detected in either mouse strains. Together, this suggests that the ablation of Panx1 does not compromise the efflux of extracellular ATP in this system during OE stimulation, possibly due to alternative pathways compensating. Notably, it appears that H100 actually stimulates less ATP release compared to the physiological condition. However, this is due to serial application of solutions and increased exposure of the OE to stimulants. Interestingly, when OE was stimulated with Pglu, there is an obvious difference in ATP release between the two populations (Panx1+/+, 3.4 ± 0.4 pM; Panx1 -/- 2.2 ± 0.3 pM; $p = 0.022$). This yields further explanation, however, we speculate that this result strongly suggests Panx1 channels contribute to ATP release during this experimental condition in particular. Given that measurements of extracellular ATP release *ex vivo* were reliable, and the Pglu condition alluded to Panx1 contribution in olfaction, similar methodological techniques were used to investigate ATP release from the VNO.

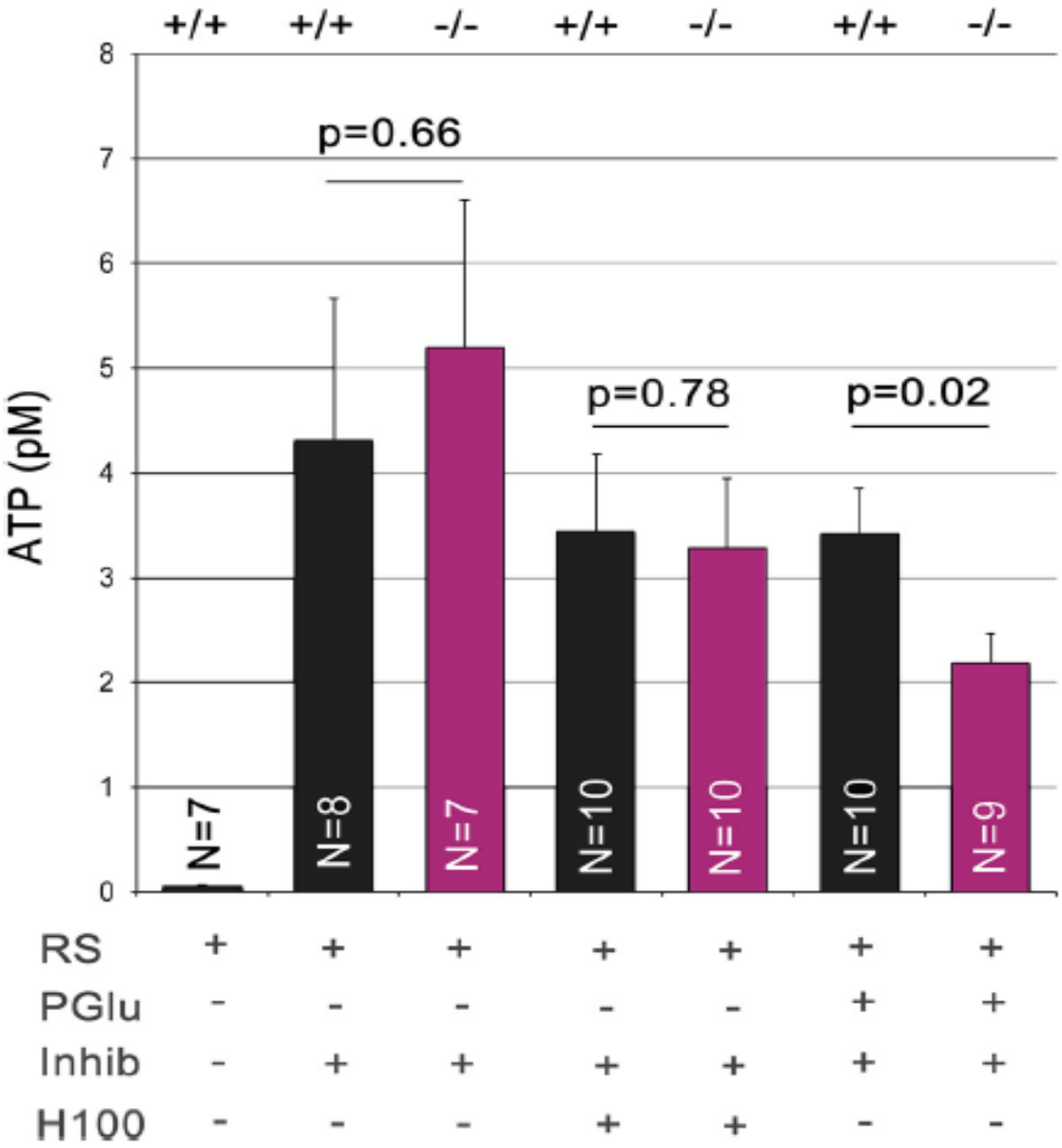

Figure 11: Quantification of extracellular ATP from the OE. Extracellular ATP was extracted from the ciliary surface of the OE after skulls from adult male mice were cut parasagittal to the septum to expose the nasal cavity. ATP concentrations were determined using this *ex vivo* preparation after serial application and complete extraction in small droplets containing Ringers solution (equilibration time: 3 min), Ringers solution with the ATPase inhibitor ARL 67156 (100 µM, equilibration time: 3 min), Henkel100 (1:1000, equilibration time: 90s). Low levels of ATP did not differ in wild type and Panx1 -/- mice. Addition of the ATPase inhibitor increased ATP levels more than 100 fold. Stimulation with Henkel100 caused significant ATP efflux in 90s. Since no differences were detectable, we concluded that alternative ATP release pathways primarily promoted ATP efflux in response to the odorant. Subsequent stimulation with potassium gluconate (Pglu, 50µM) for 90s caused a reduction in ATP release in Panx1 -/- mice, demonstrating a significant role of Panx1 channels. Error bars indicate s.e.m

4.1.5 Quantification of extracellular ATP release from the vomeronasal organ

Stimulation of ATP release in the VNO was performed mechanically. Vick and Delay (2012) had previously shown that this was possible, in order to elucidate the specific role of Panx1 in the system. We confirmed that mechanically stimulated ATP release is viable under our conditions, seeing as there were significant differences (Panx1 +/+, $p=0.01$; Panx1 -/-, $p=0.05$) in the efflux of ATP, when comparing non-stimulated Panx1 +/+ and -/- to stimulated populations for both genetic species. To our dismay, there was no significant difference seen in ATP release when we compared wild type to knock out populations. Suggesting that Panx1 has no prominent role in this setting, however, Panx3 may be contributing to function as an alternative.

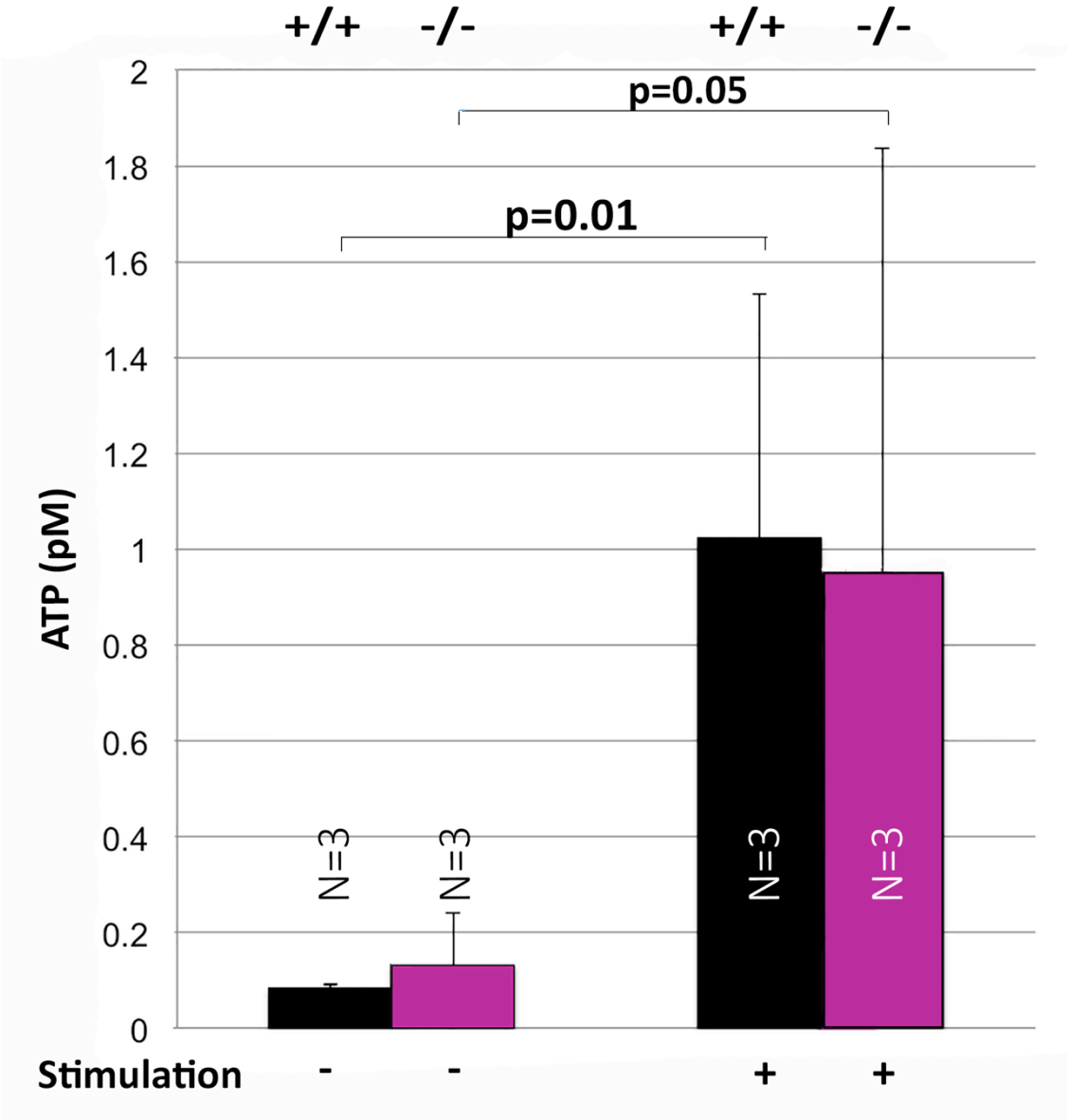

Figure 12: Quantification of extracellular ATP from mechanical stimulation of the VNO. The VNO of both Panx1 +/+ and -/- were carefully extracted and submerged in physiological Ringers solution for 3 minutes equilibration time. Ringers was carefully removed from each sample and replaced with fresh solution, when they were then subjected to either 10 minutes of mechanical stimulation, carefully generated using a pipette, or no stimulation at all. 50µL of the supernatant for each VNO was collected and 10µL was used for luminescent ATP detection assays. There is clearly no difference seen in ATP release between the 2 populations. However, there is a significant difference in ATP release in each population when mechanically stimulated (Panx1 +/+, p=0.01; Panx1 -/-, p=0.05). This demonstrates that Panx1 may not play a significant role in ATP release in the VNO as suggested. Error bars indicate s.e.m.

4.2 pH sensing: Investigating a conserved region in the Pannexin1 protein as a possible sensor of extracellular pH changes

4.2.1 Multi alignment sequence analysis

Previous research has demonstrated significant evidence for the amino acid (arginine) at position 246 being crucial to panx1 function and integrity. However, there seems to be additionally conserved amino acids in the extracellular loops of Panx1a that may be of interest to structural biologists. Using ClustalW2, it was determined that amino acids located at positions 98-105 (highlighted in red, with asterisks below showing conservation) are part of a highly conserved region in Panx1 across species (Figure 13). Of particular interest was the discovery of the histidine in the middle of this region, at location 102. Only three histidines in the entire Panx1 protein exist; H102 being the only one located extracellularly. Histidine sparks interest with chemical and structural biologists due to its pK value of approximately 6. Meaning that at physiologically relevant pH values, relatively small shifts in pH will change its average charge, causing it to protonate at pH values below 6. This property of histidine, coupled with the preliminarily established pH dependent channel functioning of Panx1, serves as a rationale for hypothesizing that the conserved region could act as an important pH sensor for the protein. Giving reason to pursue bioinformatics. Figure 14 denotes the alanine scan that was conducted on this region, in order to orient one with the position where the site-directed mutagenesis was conducted with respect to the protein as a whole.

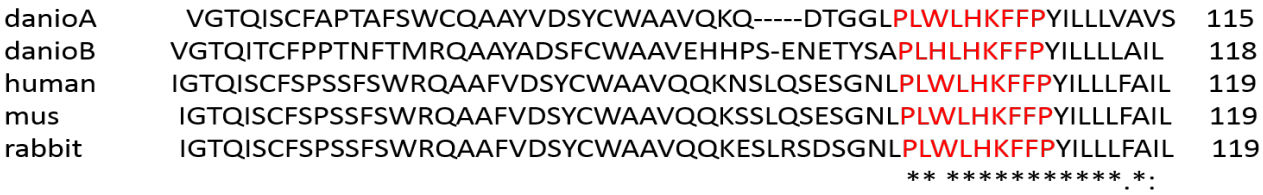

Figure 13: Multiple Sequence Alignment of Pannexin1a in Zebrafish, Humans, Rat and Rabbit. The * (asterisks) indicates positions which have a single, fully conserved residue. The : (colon) indicates conservation between groups of strongly similar properties – scoring > 0.5 in the Gonnet PAM 250 matrix. The . (period) indicates conservation between groups of weakly similar properties – scoring = < 0.5 in the Gonnet PAM 250 matrix. The amino acids that are highlighted in red are those that have been either mutated to an alanine or a histidine. (Figure adapted from http://www.ebi.ac.uk/Tools/msa/clustalw2/).

4.2.2 Structural designation of amino acid alanine mutations

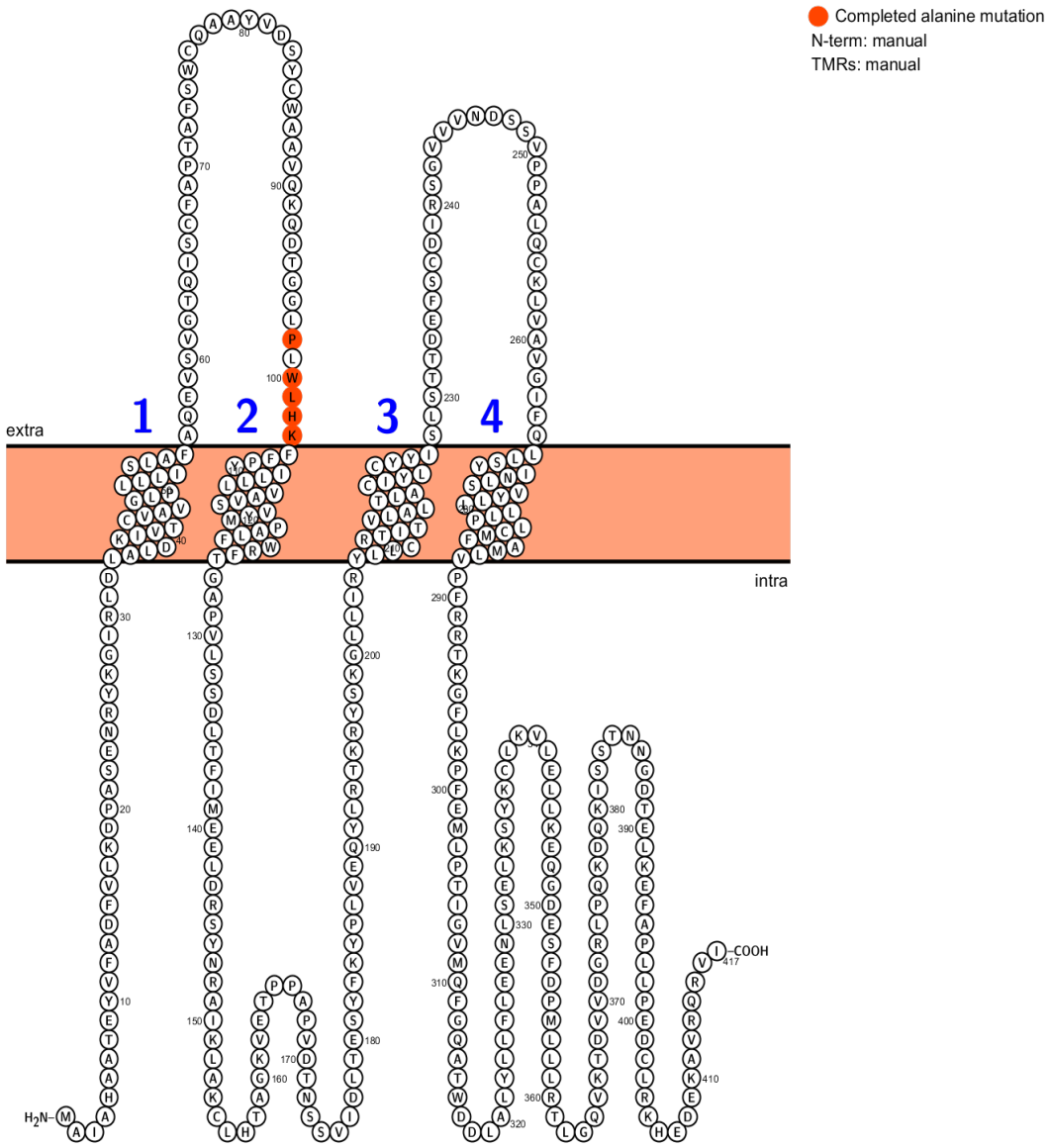

Figure 14: drPannexin1a structural denotation of alanine mutation analysis. 4 transmembrane segments are indicated, along with 2 extracellular loops, and both an amino and carboxy terminal. Highlighted in red are the amino acids (position 98, & 100 – 103) that were mutated to alanine using uniquely designed primers and the Q5 site directed mutagenesis kit.Image was created with the use of protter: http://wlab.ethz.ch/protter/start/

4.2.3 Expression of Pannexin1 protein alanine mutations

To analyze the *in vitro* expression of the alanine scan mutants, the mouse Neuroblastoma 2a (N2a) tumour cell line was used as an exogenous gene expression system, and protein expression was analyzed using western blot analysis. Whole-cell lysates were prepared from transiently transfected N2a cells of Panx1a (WT), and mutants, W100A (Tryptophan to Alanine), L101A (Leucine to Alanine), H102A (Histidine to Alanine), K103A (Lysine to Alanine), and P98A (Proline to Alanine) (Figure 15). According to the glycosylation patterns present on the western blot, the two prominent red bands around 75 kDA, we can confirm the appropriate expression of all mutants. The labelled N-glyc 1 & 2 indicates two of three glycosylation stages of the Panx1a protein, Gly1 representing the high mannose species and Gly 2 being the complex glycosylated species. N-glyc0 is likely merged with N-glyc-1. Actin is labelled in green at around 40 kDA and indicates the loading control. Meanwhile, the EYFP fusion proteins all appear at the expected weight of 74.6 kDA. These expression patterns of the mutants, the visualized double bright bands, suggest that they are properly trafficking to the membrane based upon appropriate glycosylation (Figure 15). However, in order to comment further about exact protein localization, confocal microscopy images were completed on fixed slides containing transfected cells correlating to the same mutants present in the western blot (refer to section 4.2.4).

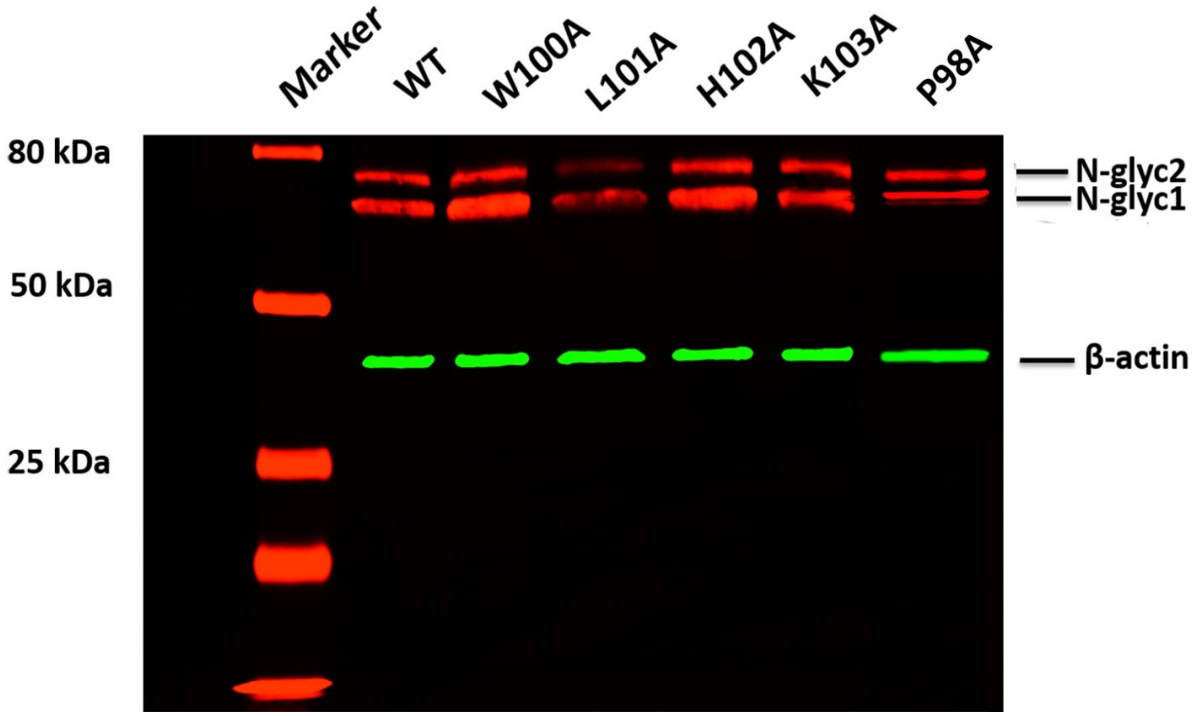

Figure 15: Western blot depicting expression of drPanx1a mutants from alanine scan analysis. N2a cells transfected with Panx1a (WT), and mutants; W100A (Tryptophan), L101A (Leucine), H102A (Histidine), K103A (Lysine), and P98A (Proline). It is important to note that P98A was conducted on a different western blot, however, all conditions were maintained. P98A was cut and imposed in photoshop. N-glyc 1 & 2 indicate 2 of 3 glycosylation stages of the Panx1a protein. N-glyc0 is likely merged with N-glyc-1. The marker is a 1kb protein ladder. Primary antibodies used include GFP 1:200 & actin 1:3000, secondary antibodies used include rb680 and m800 at 1:3000 and 1:2000 respectively. Actin is labelled in green at around 40 kDA and indicates the loading control. The EYFP fusion proteins all appear at the expected weight, 74.6 kDA. All mutants show confirmed expression and proper glycosylation patterns.

4.2.4 Localization of Pannexin1 protein alanine mutations

Confocal microscopy images depict cellular localization of the drPanx1a protein and the alanine mutants (A.a: 98, 100-103) in N2a cells (Figure 16). N2a cells were transfected with either pEYFP-drPanx1a, acting as the wild type, or 1 of 5 of the alanine mutants depicted in the western blot in figure 15. Confocal images were captured 48 h post transfection using Zeiss Confocal microscopy, adapted using ImageJ, and compiled using Photoshop. All images were taken at 63x magnification; scale depicted denotes 10µM. Dapi staining is shown in blue, depicting the nuclei, and GFP in green depicting Panx1a localization. In figure 16A, Panx1a expressing N2a cells show a confirmation of protein localization at the cell membrane with little expression in the cytosol. pEYFP-drPanx1a-P98A mutant shows ubiquitous expression, still maintaining membrane localization, with significant expression in the cytosol (Figure 16B). pEYFP-drPanx1a-W100A expresses protein localized clearly along the cell membrane and within the cytoplasm (Figure 16C). pEYFP-drPanx1a-L101A shows both membrane and cytosolic expression (Figure 16D). pEYFP-drPanx1a-H102A has full membrane expression with some expression in cytoplasmic compartments (Figure 16E). pEYFP-drPanx1a-K103A has ubiquitous expression with significant expression in the membrane, Golgi and endoplasmic reticulum (ER) compartments (Figure 16F). Overall, typical of N2a cells is their presence in populations with varying degrees of matured protein. Therefore, some of the fluorescence shown in these images located in the cytoplasm may correspond to newly synthesized proteins – localized to the ER and trafficked during protein maturation over the Golgi network to the cell surface. However, seeing as all mutations show appropriate amounts of expression in the cell membrane, there is nothing here to suggest that there should be impaired function due to improper insertion or trafficking to the membrane. Localization patterns of the mutants gave enough evidence to believe that functional analysis would be possible. Therefore, we set out to test these novel mutants under varying extracellular pH conditions using fluorescent dye uptake assays during live cell imaging.